Journal of Coastal Research	21	3	553–578	West Palm Beach, Florida	May 2005

Seasonal to Interannual Morphodynamics along a High-Energy Dissipative Littoral Cell

Peter Ruggiero†, George M. Kaminsky‡, Guy Gelfenbaum†, and Brian Voigt§

†Coastal and Marine Geology Program
US Geological Survey
345 Middlefield Road MS-999
Menlo Park, CA 94025, U.S.A.
pruggiero@usgs.gov

‡Coastal Monitoring and Analysis Program
Washington Department of Ecology
PO Box 47600
Olympia, WA 98503, U.S.A.

§University of Vermont
Rubenstein School of the Environment and Natural Resources
81 Carrigan Drive
Burlington, VT 05405-0088, U.S.A.

ABSTRACT

RUGGIERO, P.; KAMINSKY, G.M.; GELFENBAUM, G., and VOIGT, B., 2005. Seasonal to interannual morphodynamics along a high-energy dissipative littoral cell. *Journal of Coastal Research,* 21(3), 553–578. West Palm Beach (Florida), ISSN 0749-0208.

A beach morphology monitoring program was initiated during summer 1997 along the Columbia River littoral cell (CRLC) on the coasts of northwest Oregon and southwest Washington, USA. This field program documents the seasonal through interannual morphological variability of these high-energy dissipative beaches over a variety of spatial scales. Following the installation of a dense network of geodetic control monuments, a nested sampling scheme consisting of cross-shore topographic beach profiles, three-dimensional topographic beach surface maps, nearshore bathymetric surveys, and sediment size distribution analyses was initiated. Beach monitoring is being conducted with state-of-the-art real-time kinematic differential global positioning system survey methods that combine both high accuracy and speed of measurement. Sampling methods resolve variability in beach morphology at alongshore length scales of approximately 10 meters to approximately 100 kilometers and cross-shore length scales of approximately 1 meter to approximately 2 kilometers. During the winter of 1997/1998, coastal change in the US Pacific Northwest was greatly influenced by one of the strongest El Niño events on record. Steeper than typical southerly wave angles resulted in alongshore sediment transport gradients and shoreline reorientation on a regional scale. The La Niña of 1998/1999, dominated by cross-shore processes associated with the largest recorded wave year in the region, resulted in net beach erosion along much of the littoral cell. The monitoring program successfully documented the morphological response to these interannual forcing anomalies as well as the subsequent beach recovery associated with three consecutive moderate wave years. These morphological observations within the CRLC can be generalized to explain overall system patterns; however, distinct differences in large-scale coastal behavior (*e.g.,* foredune ridge morphology, sandbar morphometrics, and nearshore beach slopes) are not readily explained or understood.

ADDITIONAL INDEX WORDS: *Beach surveys, El Niño, global positioning systems, La Niña, morphology monitoring, nearshore bathymetry, Oregon State, sandbar, shoreline change, Washington State.*

INTRODUCTION

The dynamic interaction between environmental forcing and coastal morphology occurs over a wide range of time and space scales; temporal responses range from tens of seconds (wave cycles) to interannual or decadal climatic variations (El Niño Southern Oscillation and Pacific Decadal Oscillation), whereas spatial scales range from centimeters (ripples) to hundreds of kilometers (littoral cells). This range of scale presents a challenge for adequate sampling of the coastal system that must be overcome in order to provide results relevant to an improved understanding of large-scale coastal behavior and coastal management decision making.

The long-term evolution of the subaerial beach is typically of principal interest to coastal scientists and managers because of its proximity to expensive upland properties and community infrastructure. The most common measure of long-term beach change is the net migration of the shoreline over time (Figure 1), in which the shoreline position is typically defined in terms of either a proxy-based horizontal reference feature, such as the high water line delineated from topographic maps or aerial photographs (*e.g.,* CROWELL, LEATHERMAN, and BUCKLEY, 1991; DOLAN, HAYDEN, and HEYWOOD, 1978), or a datum-based shoreline extracted from ground or airborne surveys (RUGGIERO, KAMINSKY, and GELFENBAUM, 2003; STOCKDON *et al.,* 2002). A time series of shoreline position estimates is often extrapolated to predict future coastal change (DOUGLAS and CROWELL, 2000; KAMINSKY *et al.,* 1999a), and thus coastal vulnerability. However, the subaerial beach can be extremely dynamic, with the potential for tens of meters of shoreline recession or progradation occurring over periods of hours to days. Therefore, predictions of future shoreline positions are significantly enhanced with a detailed understanding of the short-term variability of beach morphology (MORTON and SPEED, 1998; RUGGIERO, KAMINSKY, and GELFENBAUM, 2003; SMITH and ZARILLO, 1990). Quantifying the seasonal to interannual var-

DOI:10.2112/03-0029.1 received 08 April 2003; accepted in revision 24 February 2004

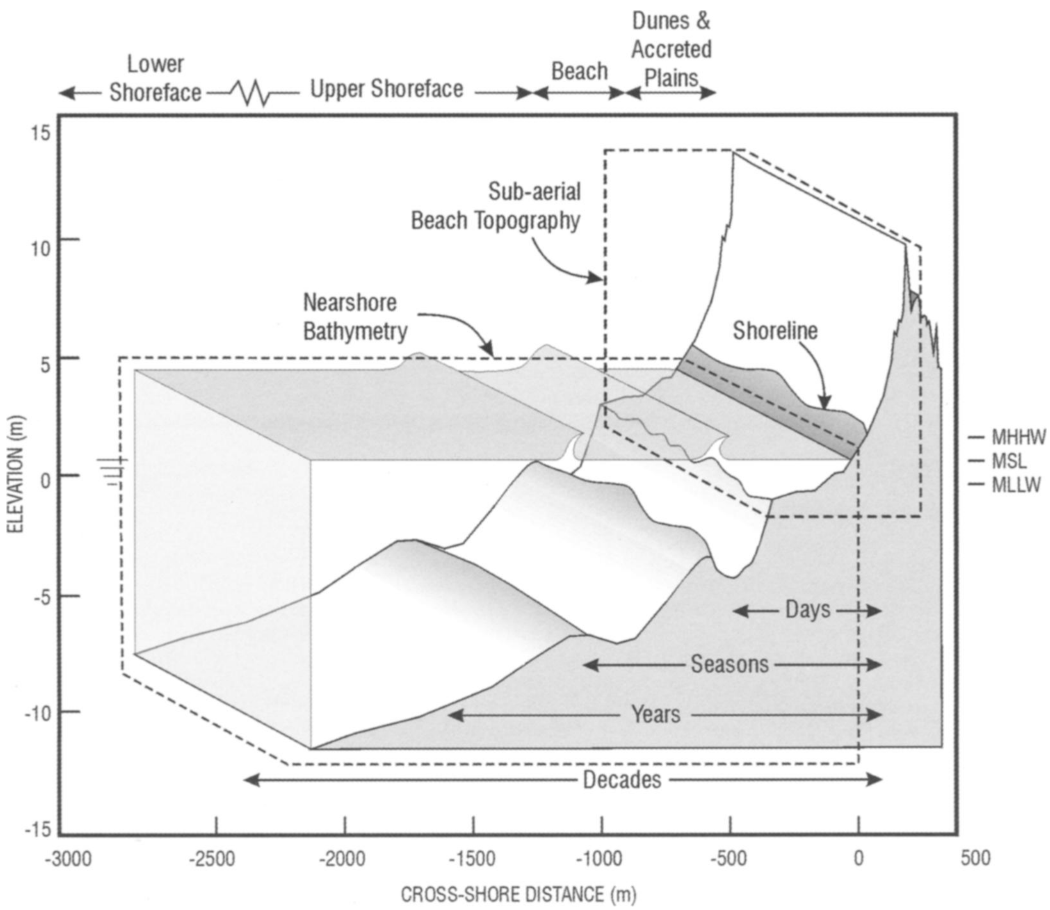

Figure 1. Conceptual diagram illustrating the motivation for a nested sampling scheme for monitoring beach change. The horizontal arrows represent approximate timescales for cross-shore morphological change. The horizontal and vertical scales shown are representative of CRLC beaches. The tidal datums mean higher high water (MHHW), mean sea level (MSL), and mean lower low water (MLLW) are shown at their approximate elevations.

iability of shoreline positions allows for the separation of long-term shoreline change trends from short-term noise when performing shoreline change analyses.

The subaerial beach, however, is only a small percentage of the active coastal zone (Figure 1). To develop reliable understanding and predictive capabilities of coastal change, knowledge of the subaqueous beach and upper shoreface variability is also necessary. Measurements within this portion of the active coastal zone are much more difficult and expensive, and relatively few large-scale long-term data sets exist worldwide (*e.g.,* the Jarkus data set along the Dutch coast; RUESSINK and KROON, 1994) and data from the Field Research Facility (FRF) in Duck, North Carolina (BIRKEMEIR, 1985; PLANT, HOLMAN, and FREILICH, 1999). Because offshore sandbars dissipate wave energy and provide a buffering capacity that protects the subaerial beach, the temporal variability of nearshore morphology (*i.e.,* position and height of sandbars and nearshore beach slope) could affect the susceptibility of the shoreline to the erosive power of waves (*e.g.,* KOMAR, 1998; RUGGIERO *et al.,* 2001). However, the large-scale behavior, both in space and time, of sandbars and nearshore morphology is just beginning to be understood.

The existing large-scale long-term nearshore morphology data sets reveal more complex behavior than originally thought to exist. For example, interannual change contributes significantly to the overall nearshore morphological variability via the slow cross-shore migration of sandbars (LIPPMAN, HOLMAN, and HATHAWAY, 1993; PLANT, HOLMAN, and FREILICH, 1999; RUESSINK and KROON, 1994; SHAND, BAILEY, and SHEPARD, 1999). This observation suggests that many existing deterministic profile change models (*e.g.,* VAN RIGN *et al.,* 2003), which assume that morphodynamic response occurs at the timescale of wave climate variability, are inconsistent with a considerable fraction of nearshore morphological variance. Other studies have shown no demonstrable link between spatial changes in environmental conditions, hydrodynamic forcing parameters or grain size, and regional differences in large-scale long-term sandbar behavior (WIJNBERG, 2002). These shortcomings are particularly serious because much of our knowledge of nearshore morphodynamics comes from experiments on the timescale of storms and poststorm recovery (WIJNBERG and KROON, 2002). However, an understanding of coastal change over interannual and decadal timescales is often most relevant to societal decisions regarding human interaction with the dynamic nearshore environment.

Many of the world's beaches exhibit significant three-dimensional beach morphology (KOMAR, 1998), implying that knowledge of the alongshore variability of the coastal planform is also important. For example, a coastal property can be fronted by a rip current that results in frequent wave impact at the toe of the dune or bluff, while only tens of meters away on either side of the rip embayment, the toe of the backshore could be buffered by a wide stable beach. Alongshore gradients in offshore sandbar position and geometry have also been hypothesized to be responsible for alternating regions of vulnerability and resilience along the coast (LIST and FERRIS, 1998; RUGGIERO *et al.,* 2001).

To effectively manage a host of complex coastal problems and make decisions on the basis of technically sound and legally defensible information, it is necessary to quantify morphological variability at multiple scales within the coastal zone. Comprehensive beach measurement programs have enhanced decision making in the coastal zones of populous states such as Florida (OFFICE OF BEACHES AND COASTAL SYSTEMS, 2001), South Carolina (GAYES *et al.,* 2001), and Texas (MORTON, 1997). These programs typically consist of topographic and bathymetric surveys (GORMAN, MORANG, and LARSON, 1998), sediment sampling (LARSON, MORANG, and GORMAN, 1997), remote sensing of shoreline positions (aerial photography or lidar), and *in situ* measurements of environmental processes such as currents, waves, and sediment transport (MORANG, LARSON, and GORMAN, 1997). Until recently, the historical trend of prograding beaches in proximity to the Columbia River in the US Pacific Northwest (Figure 2) limited the demand for coastal monitoring. Initial attempts at creating a US Pacific Northwest regional coastal database (PETERSON *et al.,* 1994) and fragmented efforts by resource management agencies were the only sources of beach morphology data for the high-energy dissipative beaches of the CRLC as of the mid-1990s.

In recent years, erosion problems have become increasingly significant throughout the CRLC and tens of millions of dollars have been spent attempting to thwart coastal erosion (KAMINSKY and GELFENBAUM, 1999). To fill the coastal processes knowledge gap, a nested, regional beach morphology monitoring program (RUGGIERO *et al.,* 1999; RUGGIERO and VOIGT, 2000) was initiated in summer 1997. The primary goal of this monitoring program is to provide morphological observations at sufficient temporal and spatial resolution to link our understanding of small-scale sediment transport processes with large-scale coastal change. The specific objectives of the monitoring program are to:

- quantify the short- to medium-term (seasonal to interannual) beach change rates and morphological variability along the CRLC and assess the processes responsible for beach change at these and other scales;
- collect beach state data (*i.e.,* grain size, beach slope, and dune and sandbar height and position) to enhance the conceptual understanding of CRLC functioning and refine predictions of future coastal change and hazards;
- compare and contrast the scales of environmental forcing and beach morphodynamics in the CRLC to other coastlines of the world; and
- provide beach change data in an appropriate format to decision makers.

In this paper, we discuss the techniques employed in the monitoring program, evaluate the sampling scheme, and present results from the first 5 years of the field campaign that quantify both the temporal and spatial morphodynamic variability of the littoral cell.

THE COLUMBIA RIVER LITTORAL CELL

The CRLC extends approximately 165 kilometers between Tillamook Head, Oregon, and Point Grenville, Washington, and consists of four concave-shaped prograded barrier plain subcells separated by estuary entrances of the Columbia River, Willapa Bay, and Grays Harbor (Figure 2). Wide, gently sloping beaches characterize the region, with sands having been derived from the Columbia River, the third largest river in the United States by discharge. Broad surf zones with multiple sandbars characterize the fully dissipative (WRIGHT and SHORT, 1983), infragravity energy-dominated nearshore zone of the CRLC. The beaches are backed predominantly by prograded dune fields and swales and by sea cliffs along the northern half of the North Beach subcell (Figure 2). The prograded barrier beaches along this tectonically active coastal margin have experienced episodic erosion (MEYERS *et al.,* 1996) and sudden subsidence events (1 to 2 meters) associated with large earthquakes of approximately 500-year recurrence intervals (ATWATER *et al.,* 1995), the last such event occurring in 1700. Anthropogenic influences, including jetty construction in the late 1800s and early 1900s at the entrances to the Columbia River and Grays Harbor (BUIJSMAN, KAMINSKY, and GELFENBAUM, 2003; GELFENBAUM *et al.,* 2001; KAMINSKY *et al.,* 1999a and b) and dam construction on the Columbia River during the 20th century (GELFENBAUM *et al.,* 1999), had a significant effect on the natural sedimentary dynamics of the CRLC coastal system.

The CRLC is well known for the severity of its wave climate (ALLAN and KOMAR, 2000, 2002; RUGGIERO *et al.,* 1997; TILLOTSEN and KOMAR, 1997), with deep-water significant wave heights and periods having annual averages of 2.2 meters and 10.4 seconds, respectively, but with winter storms generating significant wave heights of up to 14 meters (ALLAN and KOMAR, 2002). High, long-period waves (averaging ~3 meters in height and 12 to 13 seconds in period), high water levels, and a west-southwest direction of wave approach characterize the winter months (November through February), whereas smaller waves (1.2 meters and 8 seconds), lower water levels, and wind and waves from the west-northwest are the typical summer (May through August) conditions (Figure 3). Tides along the CRLC are mixed semidiurnal with a 2- to 4-meter tide range. Water levels also have a distinct seasonal cycle, measuring approximately 30 centimeters higher during the winter than during summer months (Figure 3a). At pre-

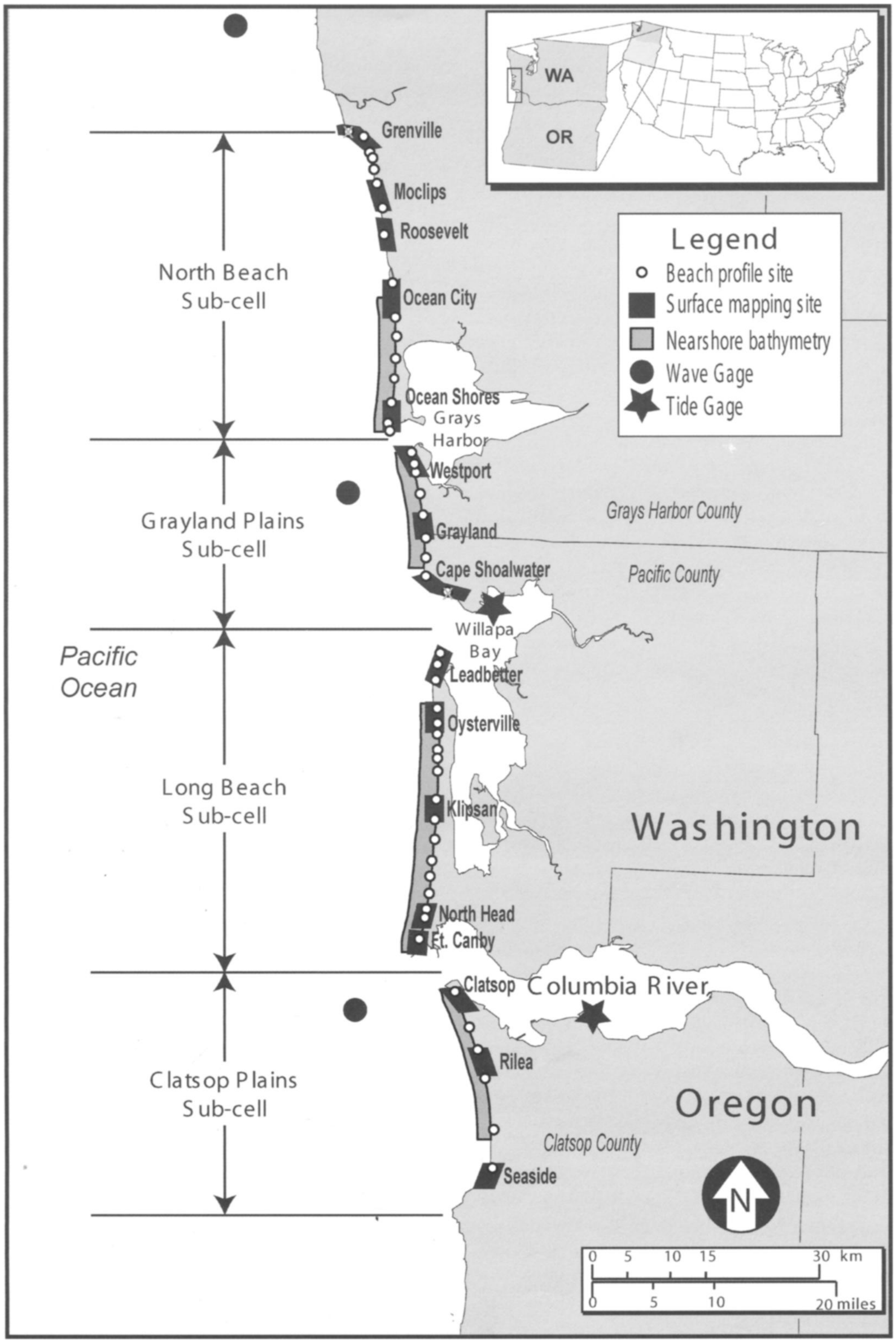

Figure 2. The CRLC cell stretches approximately 165 kilometers from Tillamook Head, Oregon, to Point Grenville, Washington. The locations of topographic beach profiles, topographic beach surface maps, nearshore bathymetric profiles, long-term tide, and long-term wave gages are shown.

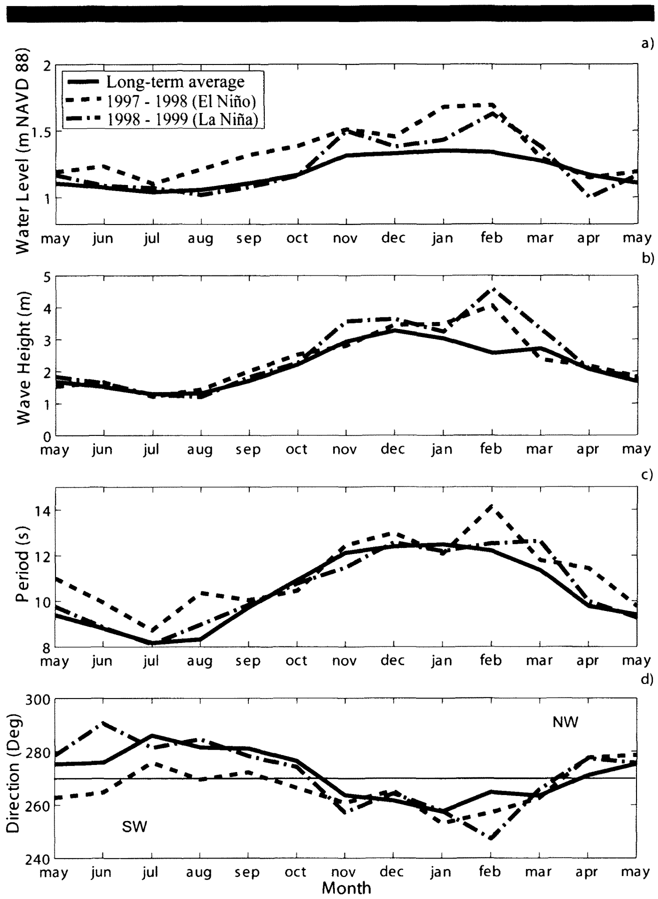

Figure 3. Monthly mean (a) water levels measured at the NOS Toke Point tide gage in Willapa Bay relative to the land-based NAVD 88 datum, (b) significant wave height, (c) period, and (d) direction from the Grays Harbor CDIP buoy. The solid line represents long-term means beginning in 1980 for water levels, 1981 for wave heights and periods, and 1993 for wave direction. The 1997/1998 El Niño (dashed line) and the 1998/1999 La Niña (dash-dot line) are also shown.

sent, three wave buoys and two tide gages operate in the CRLC (Figure 2), details of which are given in Table 1.

In the US Pacific Northwest, strong El Niños feature increased frequency of storm tracks from the south-southwest and higher than normal sea levels (KAMINSKY, RUGGIERO, and GELFENBAUM, 1998; KOMAR, 1986; KOMAR *et al.*, 2000). During the strong El Niño of 1982/1983, large wave heights and acute southerly wave angles forced an increased magnitude of offshore and northerly sand transport in Oregon, causing severe beach erosion and changes in shoreline orientation that persisted for several years (PETERSON *et al.*, 1990). The magnitude of beach change during the 1982/1983 El Niño was not documented by detailed surveys.

The beach morphology monitoring program described in this paper is one component of a much larger investigation into the regional sediment dynamics of the CRLC. The Southwest Washington Coastal Erosion Study (SWCES) is a multiscale regional investigation designed to develop an understanding of the natural processes and the human influences governing coastal change in the CRLC. The SWCES employs a hierarchical scale approach that integrates both geological investigations (*e.g.,* PETERSON *et al.*, 1999) and process measurements (*e.g.,* SHERWOOD *et al.*, 2001), scaling down from Holocene reconstruction and scaling up from process-based models (*e.g.,* KAMINSKY *et al.*, 1999). The paramount goal of the SWCES is to understand and predict the coastal behavior of the CRLC at a management scale of decades and tens of kilometers (KAMINSKY *et al.*, 1997). Data from the beach monitoring program are being integrated with long-term coastal evolution and geological framework research, to develop conceptual and predictive models of coastal evolution at scales relevant to coastal management (GELFENBAUM *et al.*, 1999; KAMINSKY *et al.*, 1999).

METHODOLOGY

The beach morphology monitoring program uses a nested sampling scheme in which multiple techniques are used to measure coastal morphology and develop knowledge of the CRLC over a range of time and space scales appropriate for decision making. Morphology monitoring is being conducted within the CRLC with a variety of real-time kinematic differential global positioning system (RTK DGPS) surveying techniques (Figure 4), widely accepted as accurate and efficient means to collect coastal morphology data (MORTON *et al.*, 1993; PLANT and HOLMAN, 1997). Components of the monitoring program include

- geodetic control,
- topographic beach profiles,
- sediment size distributions,
- topographic three-dimensional beach surface maps, and
- nearshore bathymetry.

The locations being monitored within the CRLC are distributed along each subcell to capture major geomorphic transitions, such as at jettied inlets, headlands, bluff- *vs.* dune-backed beaches, and relative changes in shoreline angle (Figure 2). The various techniques being employed are illustrated in Figure 4, and the timeline associated with the nested sampling scheme is shown in Table 2. The following sections de-

Table 1. *Characteristics of wave buoys and tide gages currently operating within the CRLC.*

Type	Station Name	Location	Water Depth (m)	Period of Operation
Waves	NDBC-46029	42°07′00″ N, 124°30′00″ W	128	1984–present
Waves	CDIP-036	46°51′24″ N, 124°14′40″ W	~40	1981–present
Waves	NDBC-46041	47°20′24″ N, 124°45′00″ W	132	1987–present
Tides	NOAA-9439040	Astoria, Columbia River, Oregon	—	1925–present
Tides	NOAA-9440910	Toke Point, Willapa Bay, Washington	—	1979–present

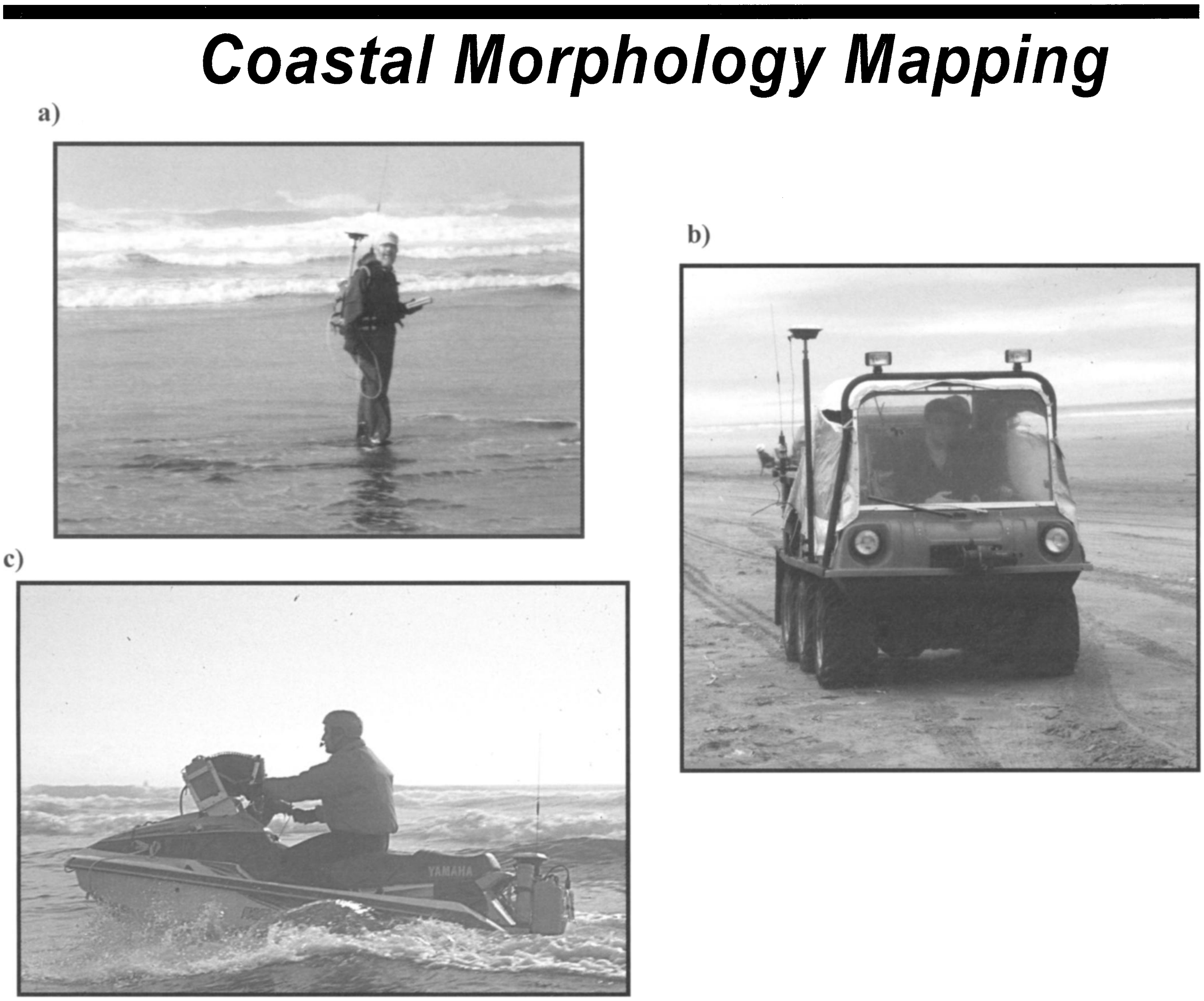

Figure 4. Real-time kinematic differential global positioning system surveying techniques used in the beach morphology monitoring program. (a) Cross-shore topographic beach profiles are collected with a rover receiver, an antenna attached to a backpack, and a hand-held data logger. (b) Three-dimensional topographic surface maps are collected with the CLAMMER. (c) Nearshore bathymetry is collected with a second-generation Coastal Profiling System.

scribe the methodologies used in the monitoring program and provide examples of the range of information provided by each component of the program.

Geodetic Control

A dense network of 76 geodetic control monuments was established in summer 1997 prior to the start of the monitoring program. Monuments were roughly located at the positions of the cross-shore topographic profiles (Figure 2) and were spaced approximately 3 to 4 kilometers apart along the coast throughout the littoral cell. The 2-centimeter-level local control network (ZILKOSKI, D'ONOFRIO, and FRAKES, 1997) was referenced to the Washington State Plane (south) North American Datum of 1983 (NAD 83) and the land-based North American Vertical Datum of 1988 (NAVD 88, which is typically within $\pm$0.2 meter of MLLW throughout the littoral cell). All subsequent data presented in this paper will be referenced to these datums. The Washington Coastal Geodetic Control Network (DANIELS, RUGGIERO, and WEBER, 1999) is being maintained over time via the replacement of damaged or destroyed monuments and station augmentation where network densification is warranted.

Topographic Beach Profiles

To resolve the seasonal to interannual variability of the subaerial beach, in two dimensions, cross-shore topographic beach profiles were collected quarterly at 47 locations along the littoral cell (Figure 2). The profiles were nominally distributed alongshore at approximately 3 kilometers, a dense enough spacing to resolve differences in beach behavior from

Table 2. *Nested sampling scheme timeline.*

Field Campaign	Geodetic Control	Topo-graphic Beach Profiles	Topo-graphic Surface Maps	Ocean Shores Monthly Surface Maps	Nearshore Bathy-metric Profiles	Sediment Samples
Summer 1997	x	x	x	x	—	x
Fall 1997	—	—	—	x	—	—
Winter 1998	—	x	x	x	—	x
Spring 1998	—	—	—	x	—	—
Summer 1998	—	x	x	x	x	x
Fall 1998	—	x	—	x	—	—
Winter 1999	—	x	x	x	—	—
Spring 1999	—	x	—	x	—	—
Summer 1999	x	x	x	x	x	x
Fall 1999	—	x	—	x	—	—
Winter 2000	—	x	x	x	—	—
Spring 2000	—	x	—	x	—	—
Summer 2000	—	x	x	x	x	x
Fall 2000	—	x	—	x	—	—
Winter 2001	—	x	x	x	—	—
Spring 2001	—	x	—	x	—	—
Summer 2001	—	x	x	x	x	x
Fall 2001	—	x	—	x	—	—
Winter 2002	—	x	x	x	—	—
Spring 2002	—	x	—	x	—	—
Summer 2002	—	x	x	x	x	x

alongshore variability in shoreline angle but too coarse a spacing to resolve smaller scale features such as beach cusps or rip current embayments. Beginning in summer 1997, profiles were collected biannually, and since fall 1998, they have been collected quarterly to better resolve the seasonal cycles of profile change (Table 2). Summer surveys were conducted in late August and September, fall surveys in December, winter surveys in late February and March, and spring surveys in June. It typically takes 10 spring low tides (approximately five full days) to complete the 47 profiles, but there can be up to several weeks between profile collection dates within any single survey campaign. By 2000, two of the original 47 profiles were eliminated, one because of poor GPS satellite visibility (profile E2) and the other because of a coastal structure and beach nourishment project (profile CSW) changing the beach environment. Two new sites, in areas warranting increased monitoring (profiles CASINO and JACKSON), replaced these locations (Figure 2, Table 3).

Beach profiles were measured by walking from the landward side of the primary foredune ridge, over the dune crest, to wading depth during a spring low tide carrying a GPS receiver and antenna mounted to a backpack (Figure 4a). The survey-grade GPS equipment used in the monitoring program have manufacturer-reported root mean square (RMS) accuracies of approximately ±3 centimeters + 2 parts per million (ppm) in the horizontal and ±5 centimeters + 2 ppm in the vertical (~4 and ~6 centimeters, respectively, for typical baseline distances) while operating in real-time kinematic surveying mode (TRIMBLE NAVIGATION LIMITED, 1998). These reported accuracies are, however, additionally subject to multipath, satellite obstructions, poor satellite geometry, and poor atmospheric conditions that can combine to cause vertical GPS drifts of as much as 10 centimeters (SALLENGER *et al.,* 2003). Local site calibrations, in which between three and five geodetic control monuments are occupied during each survey, were taken in an attempt to minimize these uncertainties. A three-parameter least squares fit was applied to adjust all data points in a particular survey to the Washington Coastal Geodetic Control System (DANIELS, RUGGIERO, and WEBER, 1999), within an RMS error typically less than 4 centimeters in the vertical, regardless of the phase of the GPS drift. Horizontal and vertical uncertainties in GPS position estimates also arose from collecting beach profiles by walking with a GPS antenna mounted on a backpack (Figure 4a). The horizontal variability between subsequent surveys was minor (~1 meter) and typically resulted in negligible vertical uncertainties because of the wide, gently sloping beaches of the CRLC (except in highly three-dimensional dune fields). Tests of the repeatability of the beach profile methodology indicated RMS vertical deviations of approximately 4 centimeters (RUGGIERO and VOIGT, 2000). Assuming that each of the components of the total vertical uncertainty are statistically independent, we combined the GPS error (~6 centimeters), the calibration error (~4 centimeters), and the repeatability error (~4 centimeters) in quadrature by taking the square root of the sum of the squares. Therefore, the beach profile methodology used in the monitoring program can only reliably detect beach elevation change greater than approximately 8 centimeters.

Although not as accurate as standard terrestrial surveying with a rod and level, walking the profiles with a GPS backpack was justified by both the reduction in survey time and the large seasonal changes observed on the high-energy beaches of the CRLC (Figure 5a). Datum-based shorelines were extracted from the beach profiles to investigate seasonal to interannual beach change (Figure 5b). Along the CRLC, the 3.0-meter (NAVD 88) contour position has been shown to most closely approximate proxy-based shorelines derived from aerial photos and maps (RUGGIERO, KAMINSKY, and GELFENBAUM, 2003). Error bars on the position of the 3.0-meter contour were calculated by the methodology described in STOCKDON *et al.* (2002) for datum-based shorelines (Figure 5b).

Sediment Samples

Sediment samples were collected at each of the 47 beach profile sites during the summer field campaigns (Table 2). Surface grab samples were collected by hand (typically several hundred grams of beach sand) at four locations along each beach profile, including the crest of the foredune ridge, at the dune toe, at midbeach, and within the swash zone at low tide. Grain size distributions were determined with American Society for Testing and Materials (ASTM)–approved dry sieves at quarter-phi intervals following US Environmental Protection Agency protocols for sediment analyses (TETRA TECH INC., 1986).

Topographic Three-Dimensional Beach Surface Maps

Whereas analyses of topographic beach profiles can reveal the cross-shore variability in subaerial beach change at one location, typically little information about the alongshore ex-

Table 3. *Beach profile names, mean contour (3.0 m) change rates, beach slopes, and mean beach grain size (D_{50}).*

Profile No.	Profile Name	Winter Retreat (m)	Summer Recovery (m)	Net Change (1997–2002) (m)	Change Rate (m/y)	Foreshore Beach Slope	D_{50} (mm)
1*†	E2	—	—	—	—	—	—
2	SOUTH	−10.9	14.9	20.0	4.0	0.014	0.125
3	L443	−23.8	31.4	45.5	9.1	0.014	0.119
4	B1	−14.8	24.7	49.4	9.9	0.012	0.126
5	A1.5	−8.1	18.5	52.2	10.4	0.013	0.129
6	PIER RM1 AZ	−10.2	17.0	34.0	6.8	0.015	0.137
7	GKAM	−15.5	16.7	5.8	1.2	0.014	0.139
8	BHUX	−2.3	−0.4	4.6	0.9	0.014	0.126
9†‡	GP-14109	—	—	—	—	0.011	0.156
10	DIANA	−20.4	19.2	−5.6	−1.1	0.014	0.139
11	DAMONS	−19.7	14.9	−23.8	−4.8	0.015	0.151
12	ET	−9.4	14.4	25.0	5.0	0.014	0.176
13	BUTTER	−17.2	23.8	32.9	6.6	0.020	0.249
14	X1 NORTH	−18.5	29.4	54.8	11.0	0.026	0.300
15	X1 SOUTH	−20.0	25.6	28.0	5.6	0.042	0.226
16	HD-1	−8.3	10.7	12.1	2.4	0.025	0.179
17	WORM	−14.4	13.6	−10.7	−2.1	0.041	0.599
18	SPICE	−3.3	0.7	−12.9	−2.6	0.053	0.714
19	RDAN	−1.4	7.4	30.4	6.1	0.030	0.209
20	PRUG	−10.2	9.2	−5.1	−1.0	0.016	0.169
21	PC068	−20.7	21.3	3.2	0.6	0.015	0.161
22†	PC064	41.1	34.2	376.3	75.3	0.012	0.165
23†	GELF	−46.3	3.7	−213.3	−42.7	0.024	0.188
24†	CSW	—	—	—	—	—	—
25†	LB1	−19.8	18.6	−5.9	−1.2	0.019	0.169
26†	PC055	3.4	29.4	164.0	32.8	0.013	0.162
27	PC051	−13.1	32.6	97.6	19.5	0.014	0.169
28	PC044	−13.7	21.8	40.6	8.1	0.016	0.171
29	PC057	−19.0	25.1	30.2	6.0	0.017	0.168
30	OYSTER 3	−15.2	22.6	36.9	7.4	0.018	0.173
31	PC037	−8.8	14.4	28.2	5.6	0.018	0.180
32	PC035	−11.3	14.6	16.6	3.3	0.018	0.185
33	PC032	−12.7	18.6	29.3	5.9	0.017	0.178
34	KLIPSAN 2	−17.6	22.0	21.7	4.3	0.018	0.196
35	PC021	−24.2	25.7	7.1	1.4	0.018	0.197
36	RICH	−20.7	24.6	19.2	3.8	0.022	0.214
37	PC014	−18.5	20.6	10.6	2.1	0.021	0.216
38	PC008	−26.4	19.6	−34.1	−6.8	0.018	0.187
39	PC025	−19.4	13.5	−29.3	−5.9	0.021	0.206
40	PC004	−17.5	13.1	−22.4	−4.5	0.025	0.206
41	CANBY	−21.8	18.3	−17.6	−3.5	0.027	0.187
42	EAST JETTY 2	−8.7	15.9	35.9	7.2	0.024	0.165
43	IREDALE	−18.9	17.6	−6.7	−1.3	0.021	0.163
44	KIM	−21.6	17.1	−13.8	−2.8	0.023	0.167
45	RILEA	−13.0	14.8	8.8	1.8	0.020	0.174
46	DELRAY	−16.8	14.6	−11.4	−2.3	0.020	0.163
47	SEASIDE RM2	−24.0	35.0	54.9	11.0	0.013	0.151
48†§	CASINO	—	—	—	—	—	—
49†§	JACKSON	—	—	—	—	—	—
	Mean	−15.3	18.4	16.1	3.2	0.020	0.196
	SD	6.1	7.5	27.7	5.5	0.008	0.107
	Maximum	−1.4	35.0	97.6	19.5	0.053	0.714
	Minimum	−26.4	−0.4	−34.1	−6.8	0.011	0.119

* Profiles 1 and 24 were discontinued in spring 1999 because of bad GPS satellite visibility and in winter 2000 because of beach fill, respectively.
† Profiles 1, 9, 22, 23, 24, 25, 26, 48, and 49 were not included in the 5-year averages.
‡ Profile 9 was affected by the northerly migration of a coastal stream in 1999.
§ Profiles 48 and 49 were begun in fall 1999 and winter 2000, repectively, and replace profiles 1 and 24.

tent of beach change can be extracted from these data. To determine both the local and regional alongshore variability in beach morphology, three-dimensional topographic beach surface maps were generated by collecting dense beach position measurements with a DGPS antenna mounted to a six-wheel-drive all-terrain vehicle (PLANT and HOLMAN, 1997) called the CLAMMER (the Coastal All-Terrain Morphology Monitoring and Erosion Research vehicle, Figure 4b). Alongshore reaches, approximately 4 kilometers in length, were mapped between the toe of the primary dune and the swash zone (typically hundreds of meters in the cross-shore direction) at 16 locations in the CRLC (Figure 2). Although these

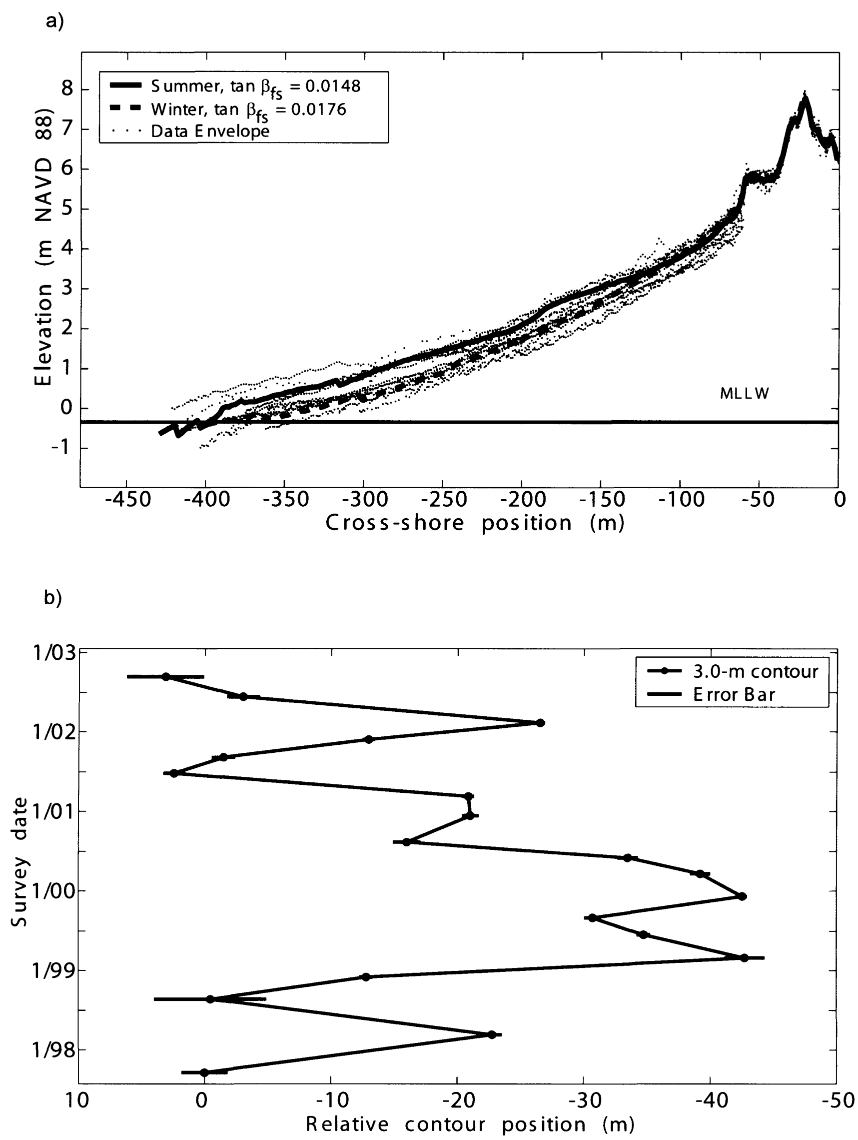

Figure 5. (a) Envelope (dots) of beach profile change at profile number 21, site PC068, in the Grayland Plains subcell between summer 1997 and summer 2002. The darker profiles represent the average summer (solid) and the average winter (dashed) beach profiles. Temporally averaged summer and winter foreshore beach slopes, tan β_{fs}, are given. (b) Time evolution of the 3.0-meter (NAVD 88) contour position and associated error bars revealing seasonal cycles and interannual reversals in trend.

surface maps provided substantially more morphological information than the cross-shore profiles, the time and expense per survey constrained the program to biannual surveys (Table 2). Three to five surface maps were collected within each subcell (Figure 2) to resolve regional gradients in beach change, and survey frequency was increased in highly dynamic areas (*e.g.,* Ocean Shores, Washington) in an attempt to determine intraseasonal changes of the beach face.

Individual point measurements composing the surface maps were densely spaced in the alongshore direction (5 to 10 meters), to resolve relatively small-scale features such as beach cusps, and extended over long enough distances to resolve larger scale, potentially migrating features such as megacusps, rip current embayments, and sand waves (Figure 6a). The cross-shore distance between alongshore transects was typically 20 to 30 meters and was determined in the field on the basis of cross-shore breaks in beach slope, crests and troughs of intertidal bars (ridge/runnel morphology), and at (rarely occurring) beach berms. The nonuniformly spaced raw data (typically 5,000 to 10,000 points per survey) were mapped onto a uniform two-dimensional gridded surface, permitting comparisons with subsequent surveys (Figure 6c). Once the CLAMMER data were gridded onto a surface (Figure 6d), datum-based shorelines (contour lines) could be ex-

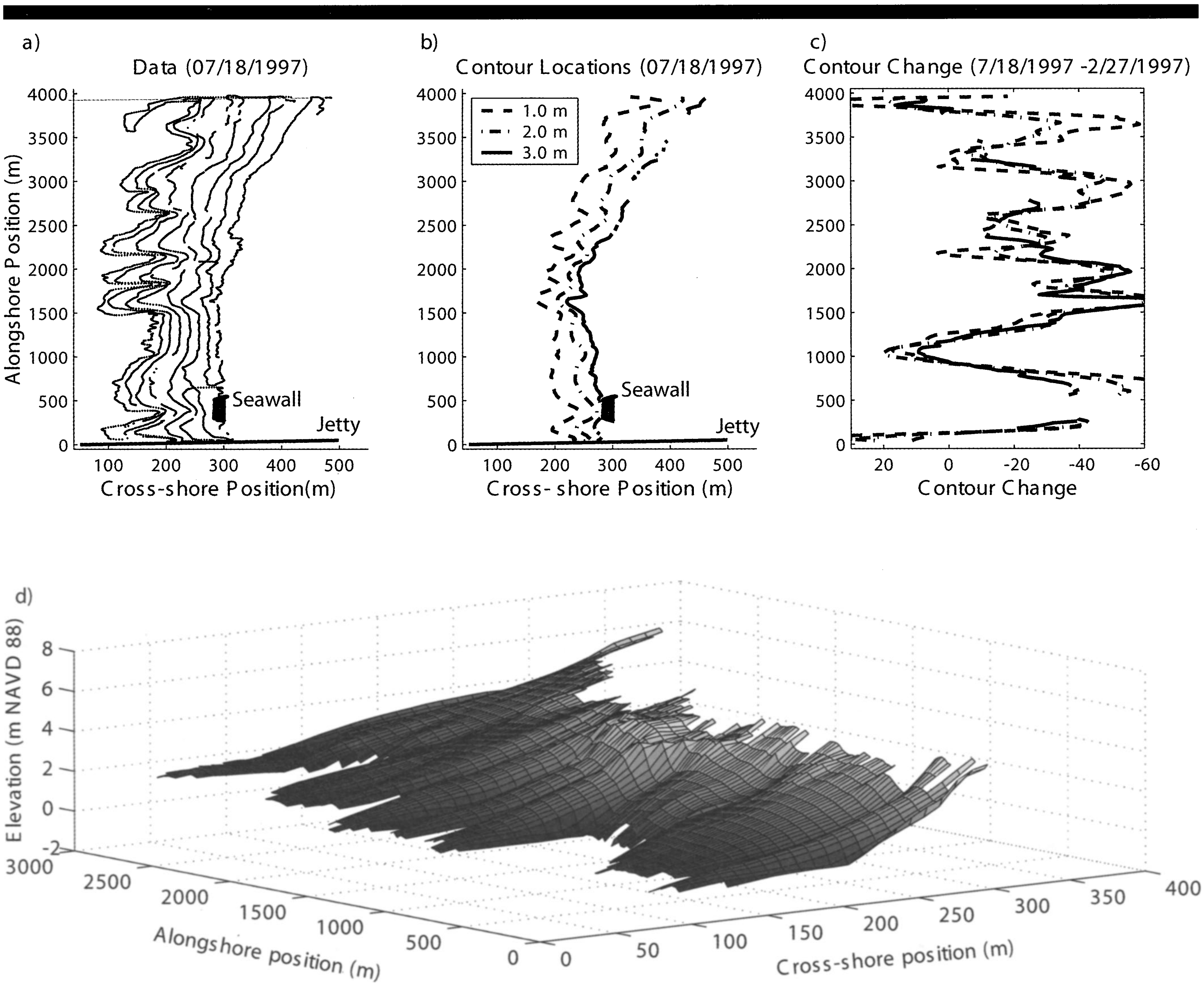

Figure 6. (a) Data coverage from the 18 July 1997 Ocean Shores surface map. The Grays Harbor North jetty and a tiered riprap seawall (wave bumpers) are also shown. (b) Contour lines (1.0, 2.0, and 3.0 meters) generated from the 18 July 1997 surface map. (c) Contour change (1.0, 2.0, and 3.0 meters) between the 18 July 1997 survey and the 27 February 1998 survey. (d) Three-dimensional beach surface map from the 18 July 1997 survey showing a megacusp/rip current embayment field.

tracted (Figure 6b). Similar to beach profile data, the individual data points within each surface map were subject to GPS system uncertainties (~6 centimeters) and calibration uncertainties (~4 centimeters). Tests showed that the vertical RMS error of the interpolated beach surface, compared with detailed beach profile surveys, was typically less than 10 centimeters.

Nearshore Bathymetry

It has historically been difficult and expensive to collect subaqueous nearshore morphology data, and only a few coastlines in the world have sufficient nearshore data to quantify the variability of this dynamic region. A second-generation Coastal Profiling System (CPSII), originally developed at Oregon State University (Beach, Holman, and Stanley, 1996; Cote, 1999; MacMahan, 2001), is being used in the CRLC (Figure 4c) to resolve the interannual variability of this high-energy nearshore planform. This system consists of a highly maneuverable personal watercraft that is equipped with an echo sounder, GPS receiver and antenna, and an onboard computer. Repeatability tests suggest subdecimeter accuracy (MacMahan, 2001); however, reasonable variations in seawater temperature (not measured) can affect depth estimates by as much as 15 centimeters in 12 meters of water.

Although some effort has been made to resolve nearshore bathymetry at intra-annual scales (Ruggiero *et al.,* 2003), the extreme waves and currents of the region and the potential danger involved in the measurement technique precludes

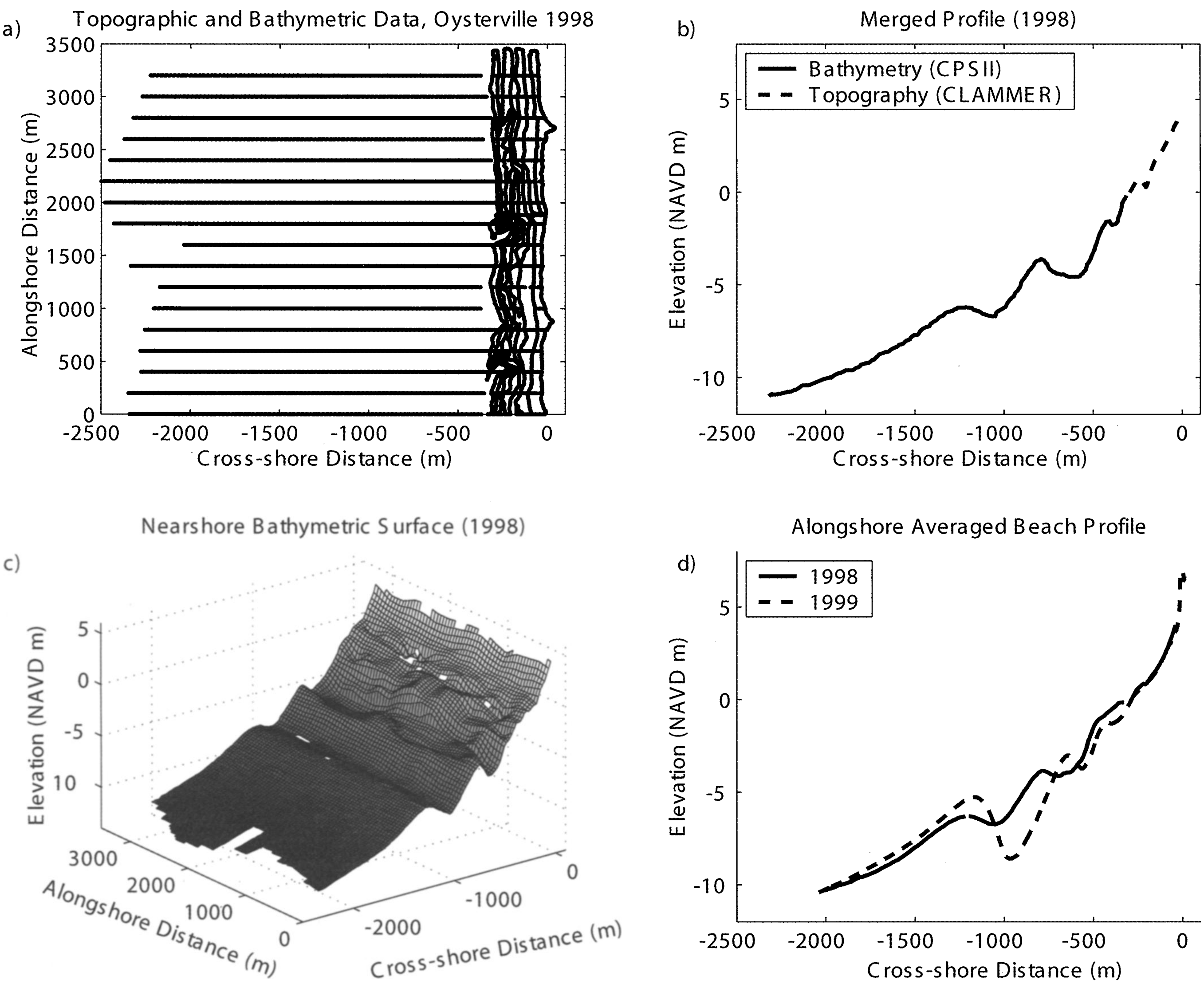

Figure 7. (a) Topographic data measured with the CLAMMER at Oysterville, Washington, is merged with nearshore beach profiles obtained with the second-generation coastal profiling system. (b) A merged profile that extends from approximately −12 meters to +5 meters (NAVD 88). (c) The complete three-dimensional nearshore planform as measured at Oysterville, Washington, in August 1998, including a linear outer sandbar in approximately 6 meters water depth and a crescentic middle bar in 4 meters of water. (d) Alongshore-averaged profiles (over a 1-kilometer alongshore distance) at Oysterville, Washington, from data of 1998 and 1999.

a detailed understanding at a regional scale of seasonal nearshore bathymetric variability. To resolve medium-scale (in space) morphological change of the nearshore planform, a section of coast (2 to 4 kilometers long) within each subcell was surveyed annually with profiles spaced at 200 meters in the alongshore (Figure 2; Ocean City, Grayland, Oysterville, and Rilea). Bathymetric data were merged with topographic data collected with the CLAMMER to produce detailed maps of the complete beach and nearshore planform (Figure 7a to 7d). Cross-shore bathymetric transects, spaced at kilometer intervals in the alongshore, were collected annually along much of the rest of the CRLC (Figure 2), revealing important information about large-scale variability in nearshore beach slopes, sandbar dimensions, and sandbar locations. Each bathymetric profile extended from approximately the shoreline to a deep-water limit ranging between 10 and 15 meters (NAVD 88).

RESULTS

The nested sampling scheme of the beach monitoring program was employed to quantify the alongshore variability of a variety of beach state parameters, as well as the short- to medium-term (seasonal to interannual) beach change rates and variability along the CRLC. Although the beach monitoring program was not specifically designed to quantify event-scale morphological response to the severe storms that characterize the region, a few localized data sets do exist. Although these limited data are not sufficient for a full understanding of the event-scale response of CRLC beaches, they suggest that morphological change due to single storms does not linearly depend only on wave conditions, but rather on a combination of waves, tides, and antecedent morphological conditions such as rip current embayments (RUGGIERO *et al.,* 1999). The following sections present regional morphometric parameters and the seasonal to interannual morphodynamic variability along the CRLC found during the first 5 years of the monitoring program, summer 1997 to summer 2002.

Beach State Parameters

Data from the monitoring program provide a regional inventory of physical parameters that help define the morphological "state" of the beach. The beaches of the CRLC are primarily comprised of well-sorted medium to fine sand with a time- and alongshore-averaged median midbeach grain size of approximately 0.20 mm (ranging from 0.12 to 0.71 mm within the littoral cell with a standard deviation [SD] of 0.11 millimeter). Extensive black-sand placer deposits exist on the beaches adjacent to the mouth of the Columbia River, accounting for up to 70% of most samples (LI and KOMAR, 1991). Although the sediments coarsen away from the source within approximately the first 10 kilometers north of the river, the general trend suggests grain sizes decrease with increasing distance from the Columbia River (Figure 8a, Table 3). This trend of alongshore sorting is interrupted near the mouth of Grays Harbor, where coarse sediment lag deposits (derived from glacial outwash and eroded from the shoreface) exist on the beach. Neglecting the two sites (WORM and SPICE) that contain this coarse sediment lag reduces the median midbeach (approximately MHW) grain size of the CRLC to approximately 0.18 millimeter.

The trend in sediment size is well correlated to a regional gradient in foreshore beach slope (Figure 8b), with slopes generally decreasing with distance from the Columbia River (correlation coefficient = 0.75, significant at the 0.05 confidence level). The slope of the subaerial beach ($\tan \beta_{fs}$) is defined as the gradient between the 1.0- and 3.0-meter elevation contours on the beach profiles. This region, typically 100 meters wide, is the most active portion of the beach face that is always measured regardless of wave and water level conditions during a particular beach profile survey. The mean foreshore beach slope in the CRLC, taken as the temporal mean of the summer values at each site, is approximately 0.020, ranging from 0.011 to 0.053 (SD = 0.008, Table 3). The northern portion of the North Beach subcell exhibits the finest grain sizes and the lowest sloping beaches within the CRLC.

Large-scale coastal behavior varies along the CRLC, as evidenced by variability in foredune ridge morphology, nearshore beach slopes, and morphometric sandbar parameters. The highest primary foredune ridges, measured in summer 1997, are in the Clatsop Plains subcell, with dune elevations measuring as high as 14 meters (NAVD 88). North of the Columbia River, foredune ridges are distinctly lower, with the lowest primary dune elevations in the northern section of the North Beach subcell, where small incipient dunes less than 5 meters (NAVD 88) have formed in front of the backing sea cliffs and bluffs (Figure 8). The cause for this variability in foredune height is probably closely linked to variability in decadal-scale shoreline change rates along the CRLC. Although the shoreline along Clatsop Plains has remained relatively stable since the 1950s (KAMINSKY *et al.,* 1999), the beaches along much of Long Beach and North Beach prograded at several meters per year during this time period. Following the conceptual model of foredune growth described by HESP (2002), stable beaches tend to build dunes vertically, whereas prograding beaches build a series of foredune ridges over time.

Sandbars are also prominent morphological features within the CRLC, and the spatial and temporal variability of sandbar properties is striking. The CRLC nearshore exhibits between zero and five distinct sandbars (typically two or three), ranging in height from approximately 0.1 meter (measurement limit) to a remarkable 6.0 meters, as measured from the seaward crest to the landward trough. Sandbar crest position varies from approximately 100 meters from the shoreline (approximated by the position of the 3.0-meter contour) for intertidal slip face ridges to over 1,000 meters from the shoreline for subtidal outer bars. The water depth at the crest of the outer sandbar ranges from −3.0 to −8.5 meters, whereas crest depths are typically −1.5 to −3.0 meters for middle bars and +2.0 to −1.5 meters for intertidal bars.

At a distance of 1,500 meters from the shoreline (approximately the seaward limit of the sandbar zone), there is approximately a 2.0 meters difference in water depth between the North Beach and Grayland Plains alongshore-averaged profiles, sites separated by only 30 kilometers (Figure 9). This vertical difference in profile translates to a difference in overall nearshore beach slope ($\tan \beta_{ns}$, calculated over the 1,500 meters seaward of the +3.0-meter contour) of 0.0058 for North Beach and 0.0081 for Grayland. The relatively shallow 1999 North Beach profile has three relatively small sandbars (Figure 9), whereas the steeper 1999 Grayland profile is virtually devoid of bars. The Long Beach profile contains three distinct sandbars, with an alongshore averaged (and thus diminished) outer sandbar 3.0 meters in height over 1,000 meters from the shoreline. The Clatsop Plains profile is the steepest of the four sites and contains a low-amplitude, large-wavelength outer sandbar approximately 1,200 meters from the shoreline and a middle sandbar approximately 2.0 meters in height. Clatsop Plains, with the steepest beach profiles, has the tallest primary foredune ridge (~14 meters) of the four subcells, twice as high as the low-sloping North Beach subcell (~7.5 meters).

Water depths 1,500 meters offshore of the shoreline, a proxy for nearshore slope, and morphometric sandbar parameters are summarized in Figure 10 for data collected during summer 2002. The water depths at 1,500 meters are relatively shallow where profiles intersect the ebb tidal deltas near the mouth of the Columbia River, Willapa Bay, and Grays Harbor. Away from estuary entrances, the nearshore slope decreases with distance from the Columbia River. Sand-

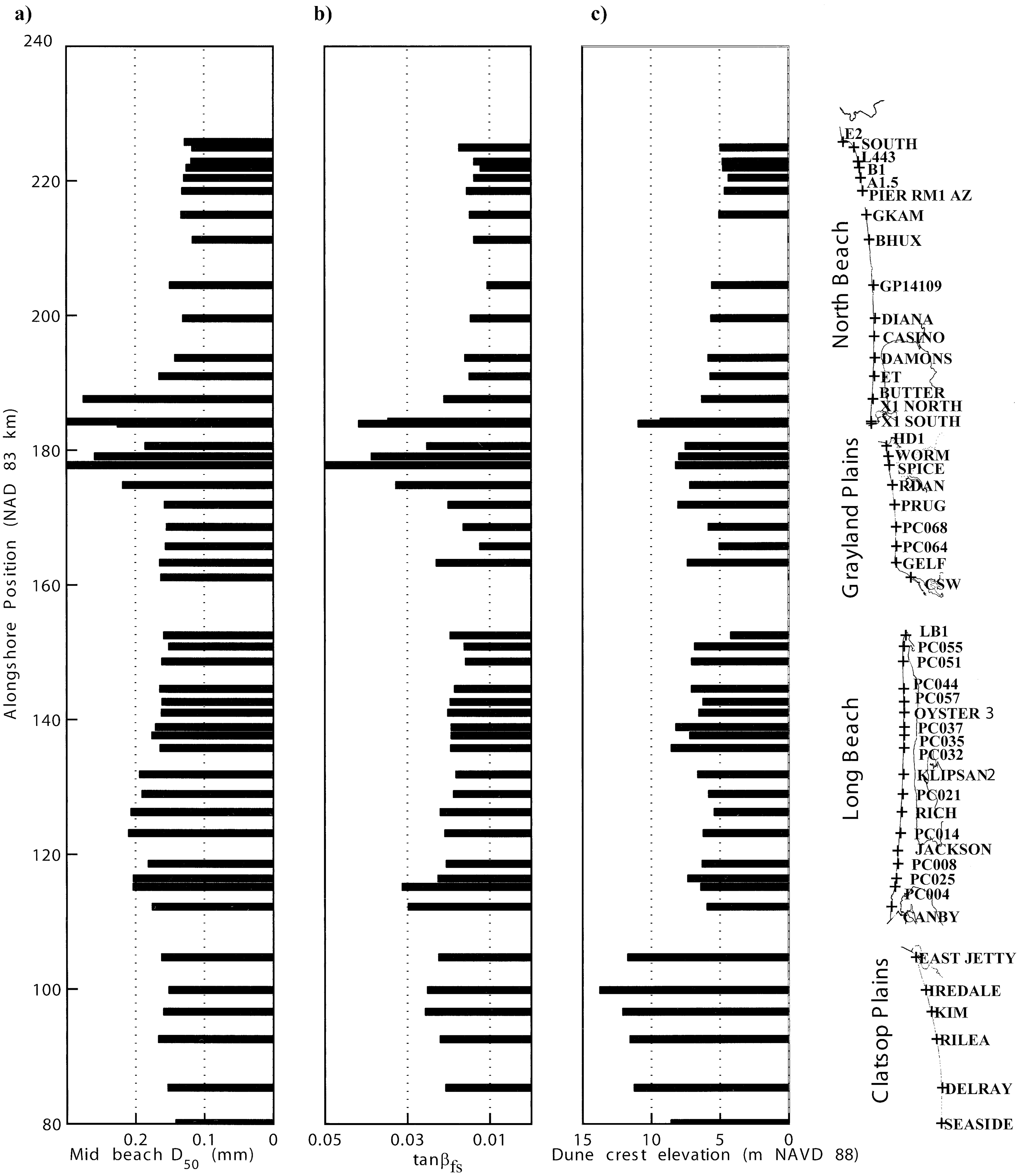

Figure 8. Beach state parameters along the CRLC. (a) Average median grain size from samples collected at approximately MHW during the summer. (b) Slope of the subaerial beach, defined as the gradient between the 1.0- and 3.0-meter elevation contours on the profile. Slope values are averages from the six summer surveys collected since 1997 at each of the 47 beach profile locations. (c) Primary dune crest elevation, as measured in summer 1997, relative to NAVD 88.

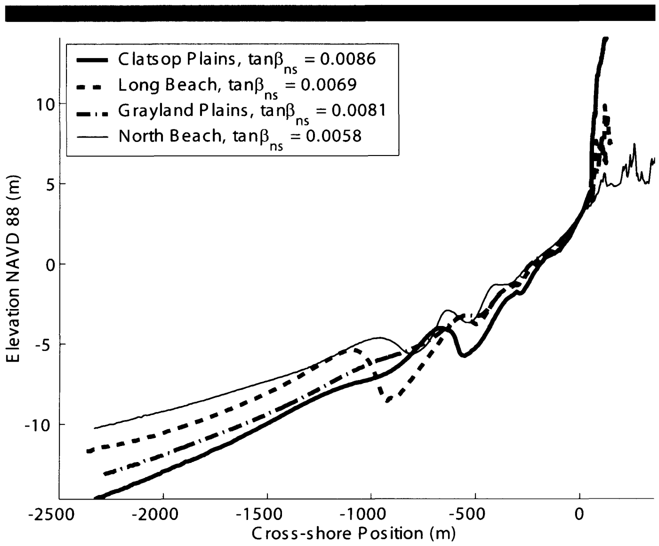

Figure 9. A comparison of alongshore-averaged profiles (averaged over 1 kilometer) collected in 1999 from each of the medium-scale (2–4 kilometers alongshore) nearshore bathymetric study sites. Each profile, averaging 10 individual transects, has been translated horizontally so that the 3.0-meter contour (NAVD 88) is at a cross-shore position of 0.0 meters, allowing for intersite comparisons of beach slopes and sandbar properties.

bar behavior along Long Beach is different from that along the other subcells, in that the outer sandbar is further from the shoreline and in deeper water (Figure 10b and 10c). The 2002 Long Beach middle sandbar is larger in amplitude than any other bars within the CRLC. Along the southern 10 kilometers of Long Beach, there is a relationship between nearshore beach slope and outer sandbar position, with steeper beaches (deeper water at 1,500 meters) having outer bars further from the shoreline (Figure 10a and 10b).

Seasonal Climate and Beach Change Variability

The seasonal cycle in waves and water levels along the CRLC (Figure 3) force a seasonal cycle in beach morphodynamics, with offshore and northerly sediment transport resulting in beach erosion during the winter and onshore and weak southerly sediment transport dominating beach recovery in the summer months (RUGGERO *et al.,* 2003; SHERWOOD *et al.,* 2001). Between summer 1997 and winter 1998, the subaerial beach face lowered an average of approximately 0.4 meter (ranging from an elevation gain of 0.4 meter to a lowering of 1.7 meters, SD = 0.4 meter) and retreated horizontally, at the 3.0-meter contour, approximately 19 meters (ranging from 11 meters of advance to 71 meters of retreat, SD = 17 meters; Figure 11). During the first winter of the monitoring program, the subaerial beach lost an average of approximately 70 m^3/m of beach sand (ranging from 60 m^3/m of volume gain to 230 m^3/m of volume loss, SD = 60 m^3/m) to the offshore. The average horizontal retreat of the shoreline for the profiles during each winter season of the monitoring program, as well as the average horizontal recovery during each summer season, is listed in Table 3.

A three-dimensional topographic beach surface map collected nominally monthly since August 1997 at Ocean Shores, Washington (Figure 2), resolves the seasonal cycles of beach change at the southern end of the North Beach subcell. Data from each of the monthly 4-kilometer surveys, over 40 individual surveys as of summer 2002, are aggregated into statistics that, when compared with the results of subsequent surveys, are robust indicators of relative beach change. Beach changes at Ocean Shores are dominated by a seasonal periodicity with beach retreat in the winter and progradation in the summer, as evidenced by the alongshore-averaged time evolution of the 3.0-meter contour (Figure 12). This seasonal morphological signal is equally well correlated with the seasonal cycle in mean wave power and wave height (correlation coefficient is approximately 0.6 for both relationships, significant at the 0.05 confidence level).

Within each of the 4-kilometer-long surface maps there is often substantial alongshore variability in beach morphology. Figure 13a suggests that since 1997, the beach within a kilometer of the Grays Harbor North jetty (kilometer 1) has behaved in a slightly different manner than the beach 3 kilometers to the north (kilometer 4), although the general trend is similar. Closest to the jetty, the shoreline was usually 15 to 20 meters landward, relative to its 1997 position, of the shoreline 3 kilometers to the north. In particular, the beach at kilometer 1 recovered earlier than the beach at kilometer 4 during spring 1998 and eroded later during winter 1999. The standard deviation of the 3.0-meter contour position can be used as a measure of alongshore morphodynamic variability. This parameter ranges from approximately 15 to 30 meters over the 4-kilometer reach (Figure 13b). The relatively stable section of coast at the alongshore position of 400 meters (approximately 400 meters north of the Grays Harbor North jetty) is the location of a persistent rip current, where the beach is often armored by a thin layer of gravel and has a steeper foreshore slope than the beaches to the north and south. At least within the first kilometer north of the jetty, the standard deviation of the contour position is negatively correlated with the average foreshore beach slope (Figure 13b).

The remaining 15 topographic surface map sites along the CRLC (Figure 2) have been surveyed at least biannually since 1997. The alongshore-averaged horizontal beach retreat of the 3.0-meter contour for the entire littoral cell during the winter is approximately 18 meters (ranging from 6 to 36 meters of retreat, SD = 7 meters; Figure 14). The average summer recovery is approximately 20 meters (ranging from 11 to 29 meters of recovery, SD = 6 meters). As a result of the seasonal reversals in cross-shore and alongshore sand transport directions, the net change of the 3.0-meter contour position over the full annual cycle is often small relative to the seasonal variability.

Seasonal variability in nearshore beach profiles has been measured at only one location because of the difficulty of nearshore bathymetric surveying during the severe nonsummer months. During spring 2001, repeated morphology measurements were made at Ocean Shores, Washington, as part of the Grays Harbor sediment transport experiment. During this period, mild wave conditions induced onshore-directed

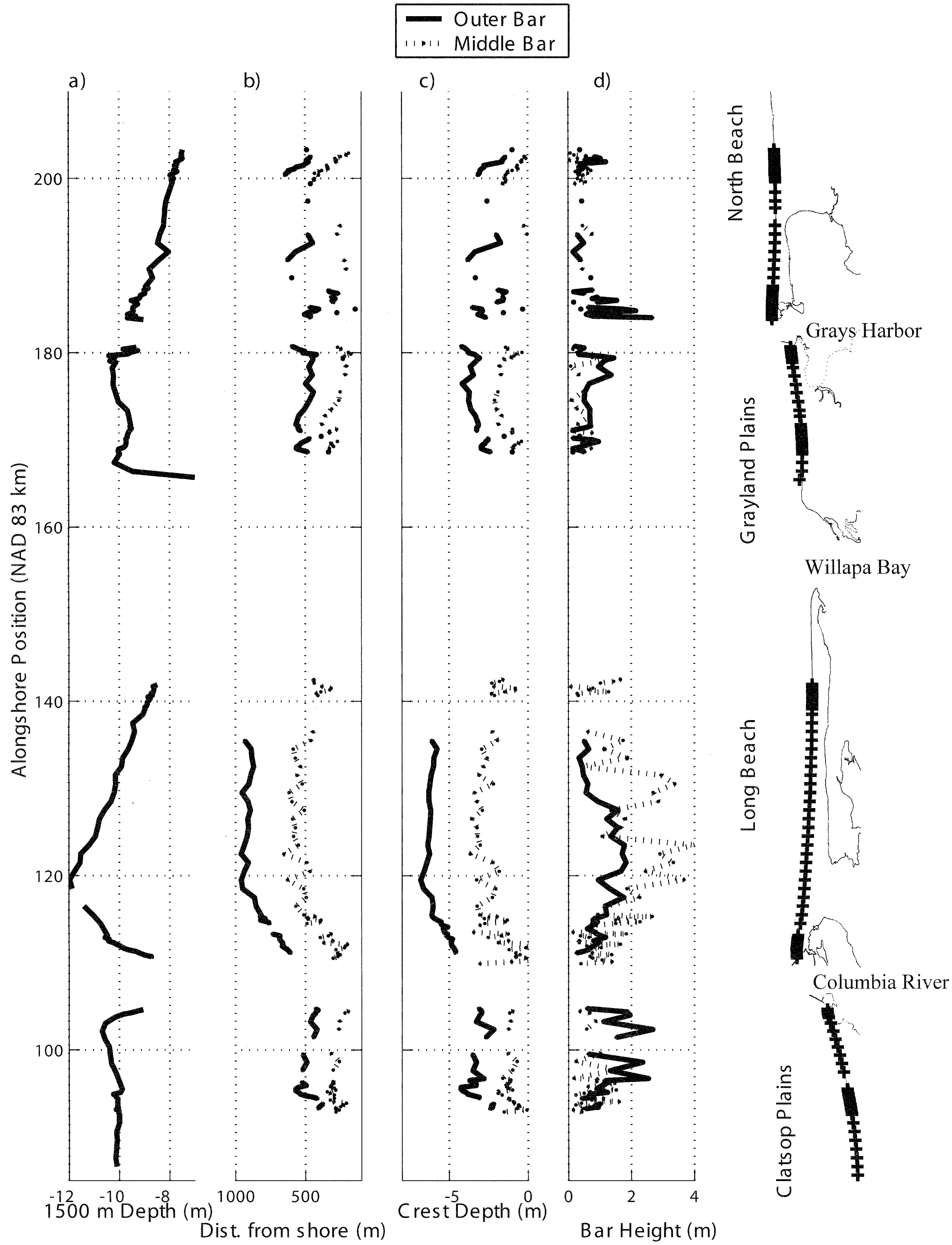

Figure 10. Bathymetric beach state parameters (summer 2002). (a) Water depth at 1,500 meters from the 3.0-meter contour, (b) position of sandbar (outer and middle) crests, (c) sandbar crest depths, and (d) sandbar heights. The plusses on the map of the littoral cell indicate where nearshore beach profiles were collected.

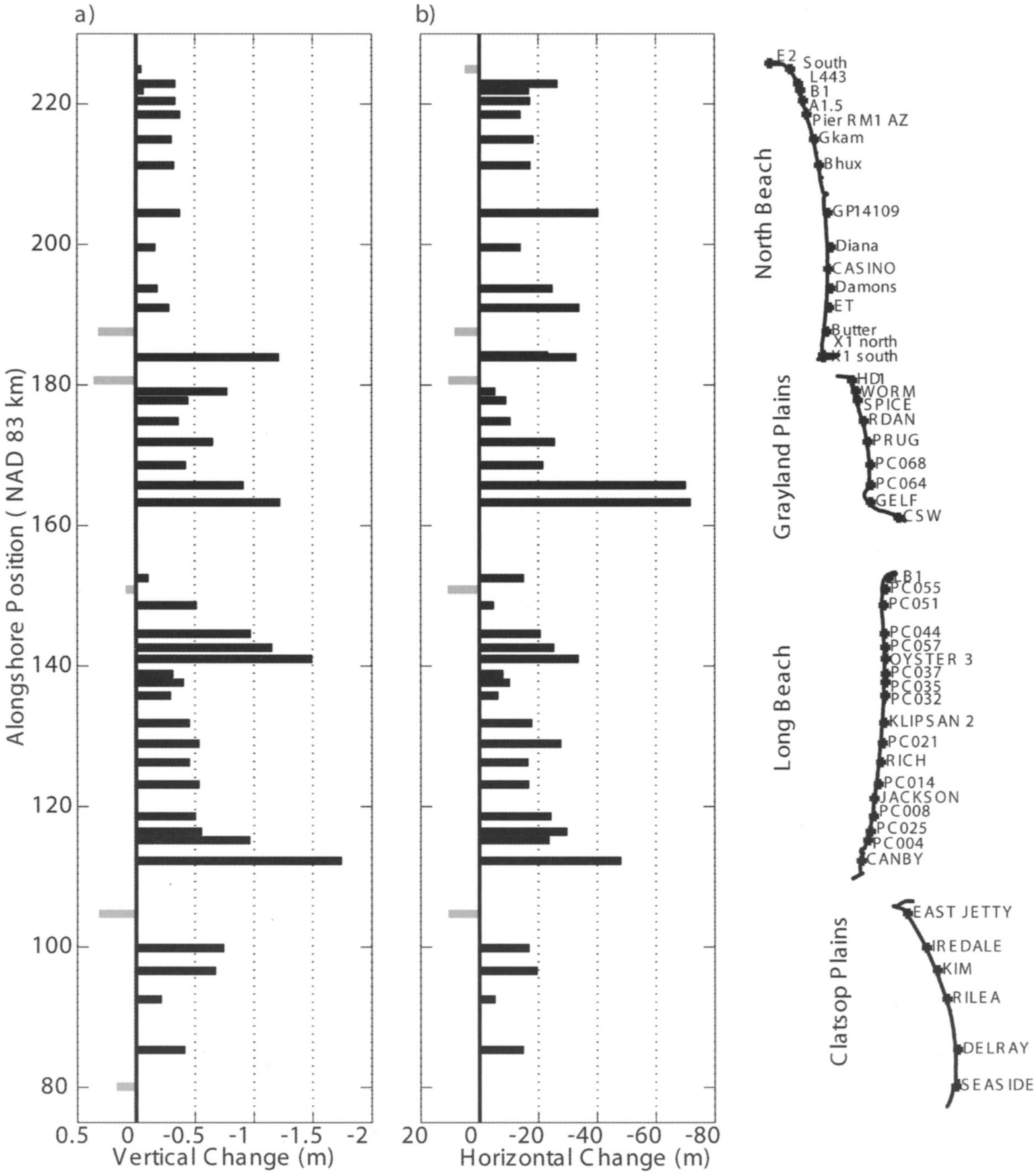

Figure 11. (a) Vertical beach change, averaged between the 1.0- and 4.0-meter contours, and (b) horizontal beach change, 3.0-meter contour, between summer 1997 and winter 1998. Positive values are accretion (progradation) and negative values are erosion (recession).

bedload transport, which resulted in shoreline progradation between April and July. The outer sandbar at Ocean Shores migrated onshore approximately 100 meters, as sand, scoured from the seaward flank of the winter bar, was deposited in the landward trough producing vertical profile changes of approximately 1 meter (not shown). The overall height of the outer sandbar decreased from approximately 2 meters to less than 1 meter, while the shoreline prograded as much as 20 meters (Ruggiero *et al.,* 2003).

Interannual Climate and Beach Change Variability

Interannual climatic variability affects waves and water levels, which in turn can influence beach responses. The win-

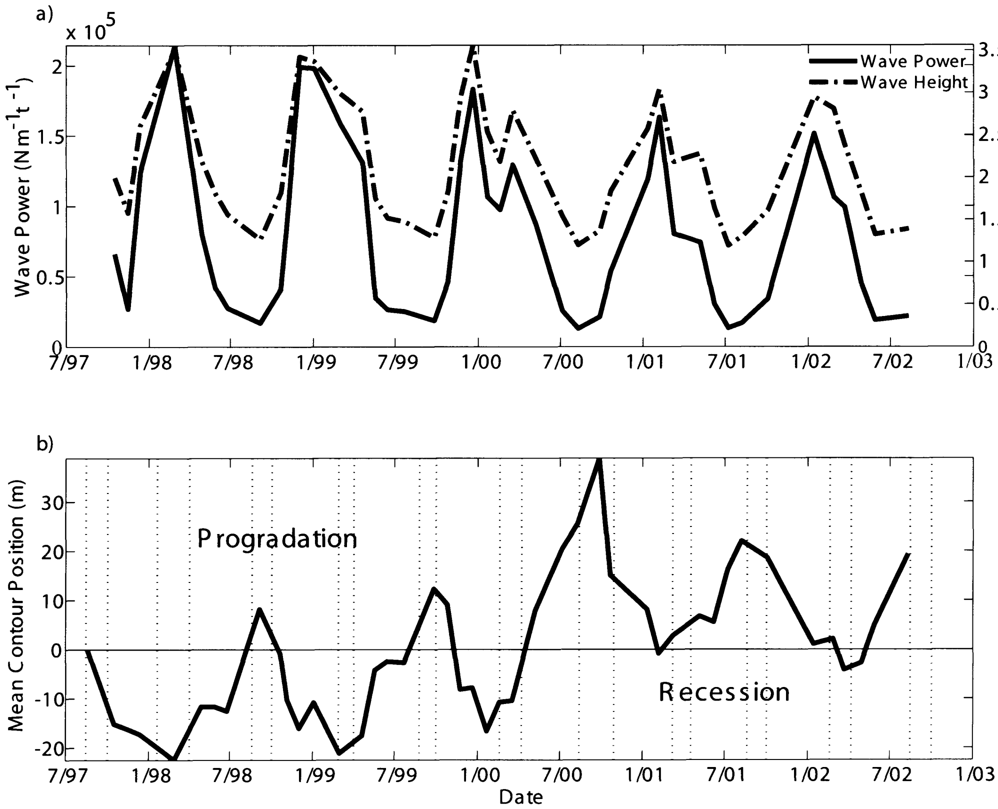

Figure 12. (a) Monthly mean wave power and wave height from the Grays Harbor CDIP buoy and (b) interannual beach change at Ocean Shores, Washington, is represented as the time history of the location of the alongshore-averaged 3.0-meter contour position relative to the August 1997 baseline data set. The vertical dotted lines represent the beginning and end of the seasonal, summer and winter, survey campaigns for the entirety of the CRLC.

ter of 1997/1998, the first winter of the monitoring program, coincided with one of the strongest El Niño events on record for the US Pacific Northwest (KOMAR *et al.,* 2000). The time evolution of the 3.0-meter contour from beach profiles at the southern and northern ends of each subcell reveals the effect of the El Niño conditions on beach change (Figure 15). In each case, the profile in the northern part of the subcell prograded relative to the profile in the south. This pattern, beginning during the El Niño winter, persisted for several years following the event. At profiles HD-1 (Grayland Plains) and EAST JETTY 2 (Clatsop Plains), the 3.0-meter contour actually prograded during the winter of 1997/1998 because of the impounding effect the nearby jetties (Grays Harbor South jetty and Columbia River South jetty, respectively) had on northward-directed sediment transport. Along the North Beach subcell, a pulse of sediment appeared on the northern beaches following the summer of 1999, presumably from the northerly transport of sand eroded from beaches to the south. The Long Beach subcell experienced net erosion in the south, whereas the beaches to the north experienced persistent progradation. The alongshore spacing of the three-dimensional beach surface maps clearly resolved the effect of the 1997/1998 El Niño on the region's beaches. Figure 16 shows the 3.0-meter contour change rate from summer 1997 to summer 1998 calculated from 15 of the 16 surface maps (the Cape Shoalwater site is not shown because it is within the entrance to Willapa Bay and dominated by inlet processes). Each subcell shows maximum net erosion or minimum net accretion at the southern end of the subcells (except in the North Beach subcell, where these extremes occur closer to the middle of the subcell) and maximum net accretion at the northern subcell boundaries. Each subcell shoreline realigned, presumably in response to the acute southerly wave directions associated with the 1997/1998 El Niño.

A moderate La Niña event in 1998/1999 immediately followed the El Niño of 1997/1998. By summer 1999, the end of the second year of the monitoring program, approximately 60% (24 of the 40 profile locations not dominated by inlet processes) of the beach profile sites within the CRLC experienced net recession of the 3.0-meter contour. The average rate of change during this 2-year period for all locations was approximately 2.7 m/y of shoreline recession. Many of the surface map sites (53%, 8 of 15, not including Cape Shoalwater) also documented significant net shoreline change over this 2-year period, averaging 3.3 m/y of recession.

Relative to the El Niño year of 1997/1998 and the La Niña year of 1998/1999, the winters of 1999/2000, 2000/2001, and 2001/2002 were moderate, with water levels, wave heights, and wave periods close to the long-term averages (Figure 3). The beaches of the CRLC recovered during these 3 years of

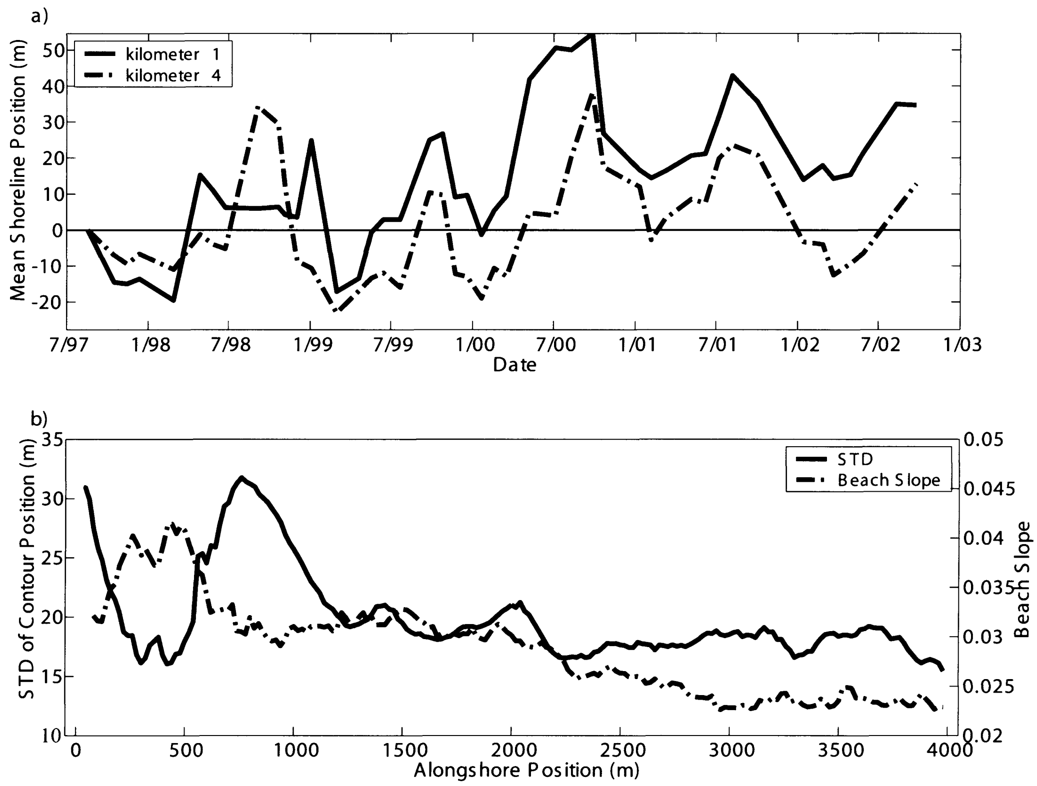

Figure 13. Alongshore variability of Ocean Shores monthly surface map shown via (a) differences in shoreline evolution close to the Grays Harbor North jetty (kilometer 1) and 3 kilometers to the north (kilometer 4) and (b) the alongshore variability of the standard deviation of the 3.0-meter contour position and subaerial beach slope.

moderate environmental forcing. By summer 2002, the end of the fifth year of the monitoring program, 70% (28 of 40) of the beach profile sites experienced net progradation. The average rate of change during this 5-year period, calculated from the profiles, was approximately 3.2 m/y of shoreline (3.0-meter contour) progradation. During this same time period, 60% (9 of 15) of the beach surface maps also demonstrated progradation, averaging 2 m/y of net progradation (ranging from 7 m/y of retreat to 23 m/y of progradation, SD = 7 m/y; Table 4). Although the majority of beaches are net prograding, several sites experienced significant net erosion during the 5 years of observations. Portions of the Clatsop Plains eroded at an average rate of over 4 m/y, and the southern Long Beach Peninsula eroded at average rates of up to 6 m/y (Table 4).

Annual nearshore bathymetric surveys along the CRLC typically reveal large redistributions of sediment in the cross-shore, consisting primarily of the growth and migration of sandbars (Figure 7d). Sandbars along the Long Beach subcell migrated offshore between 1999 and 2002 in a manner similar to that observed on several other coasts (Plant, Holman, and Freilich, 1999; Ruessink and Kroon, 1994). Net offshore sandbar migration is thought to follow a three-stage process: sandbar generation near the shoreline, seaward migration, and sandbar degeneration in the outer nearshore (Shand, Bailey, and Shepard, 1999). A probable interpretation of sandbar behavior along Long Beach (Figure 17) is that the 1999 outer sandbar migrated offshore and degenerated before the summer 2000 survey, marking the endpoint of this three-stage process. The outer sandbar in 2000 is probably the same morphological feature as the inner sandbar in 1999, a feature that did not migrate seaward during the moderate wave year of 1999–2000. Shand, Bailey, and Shepard (1999) proposed that the duration of this three-stage process increases with lower sloping beaches and higher wave energy. This would suggest that the next disappearance of the outer sandbar along the CRLC might not occur for several more years. However, the outer sandbar has already migrated several hundred meters offshore and decreased in amplitude since 2000 (Figure 17). Continued field efforts will be aimed at addressing the similarities and differences between net offshore sandbar migration along the CRLC and other coasts exhibiting this behavior.

DISCUSSION

Morphodynamic Classification

Wright and Short (1983, 1984) synthesized the variability of Australian beaches and proposed a continuum of morphodynamic beach states, with two end-member extremes, fully dissipative and highly reflective, and four commonly occurring intermediate states. Surf scaling parameters (*i.e.,* ϵ; Guza and

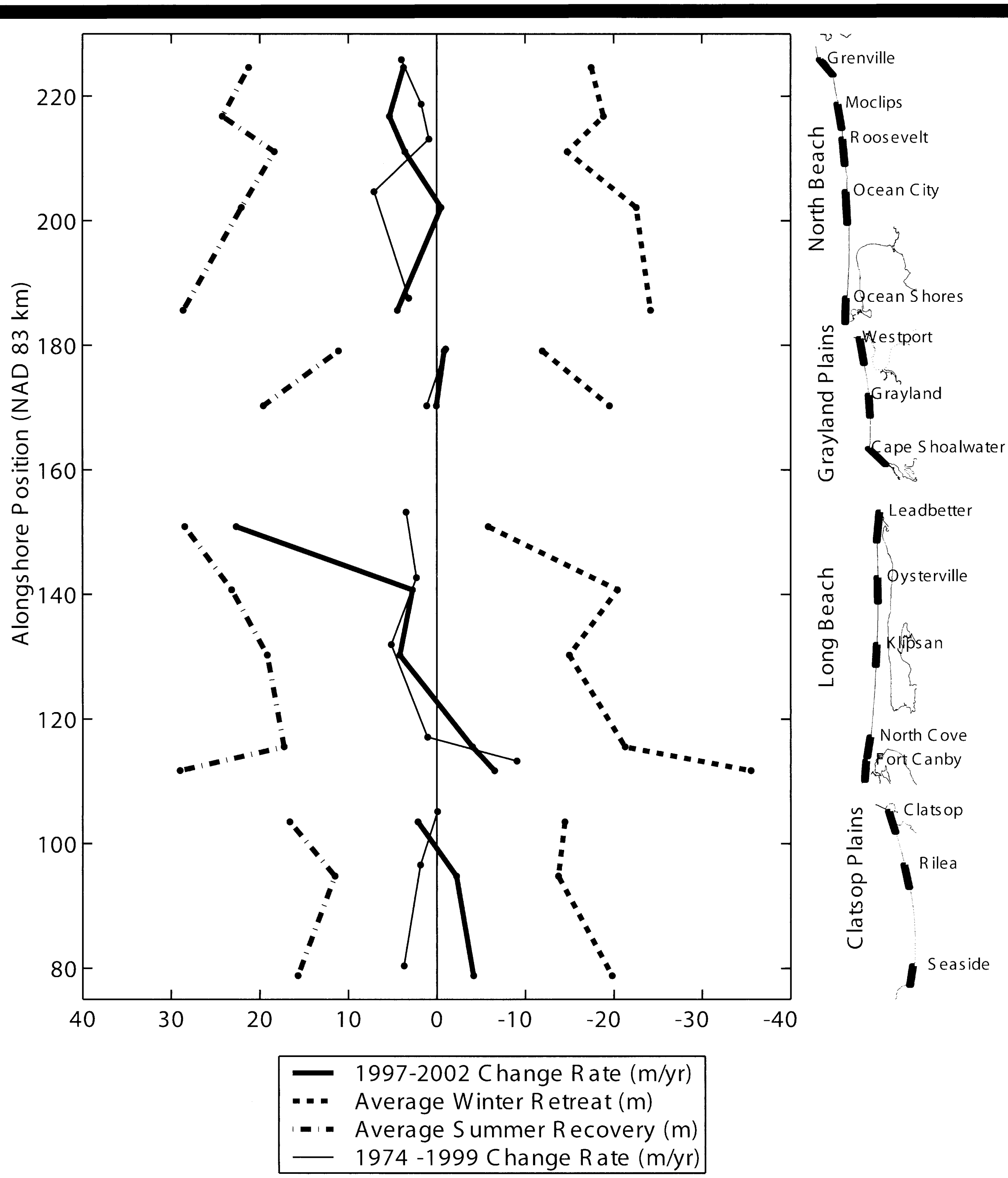

Figure 14. Seasonal-interannual variability, average winter erosion, and average summer progradation of the 3.0-meter contour line (shoreline) derived from 15 of the 16 beach surface maps between 1997 and 2002. Also shown are the longer term (1974–1999) shoreline change rates as derived from aerial photographs.

INMAN, 1975), parameters that combine wave and sediment characteristics (*i.e.,* Ω; DEAN, 1973), and parameters that quantify the relative importance of tidal range (*i.e.,* RTR; MASSELINK and SHORT, 1993) have been proposed to distinguish where beaches fall on this morphodynamic continuum.

$$\epsilon = (H_b/2)\omega^2/g \tan^2\beta \quad (1)$$

$$\Omega = H_b/(\bar{\omega}_s T) \quad (2)$$

$$\mathrm{RTR} = \mathrm{MSR}/H_b, \quad (3)$$

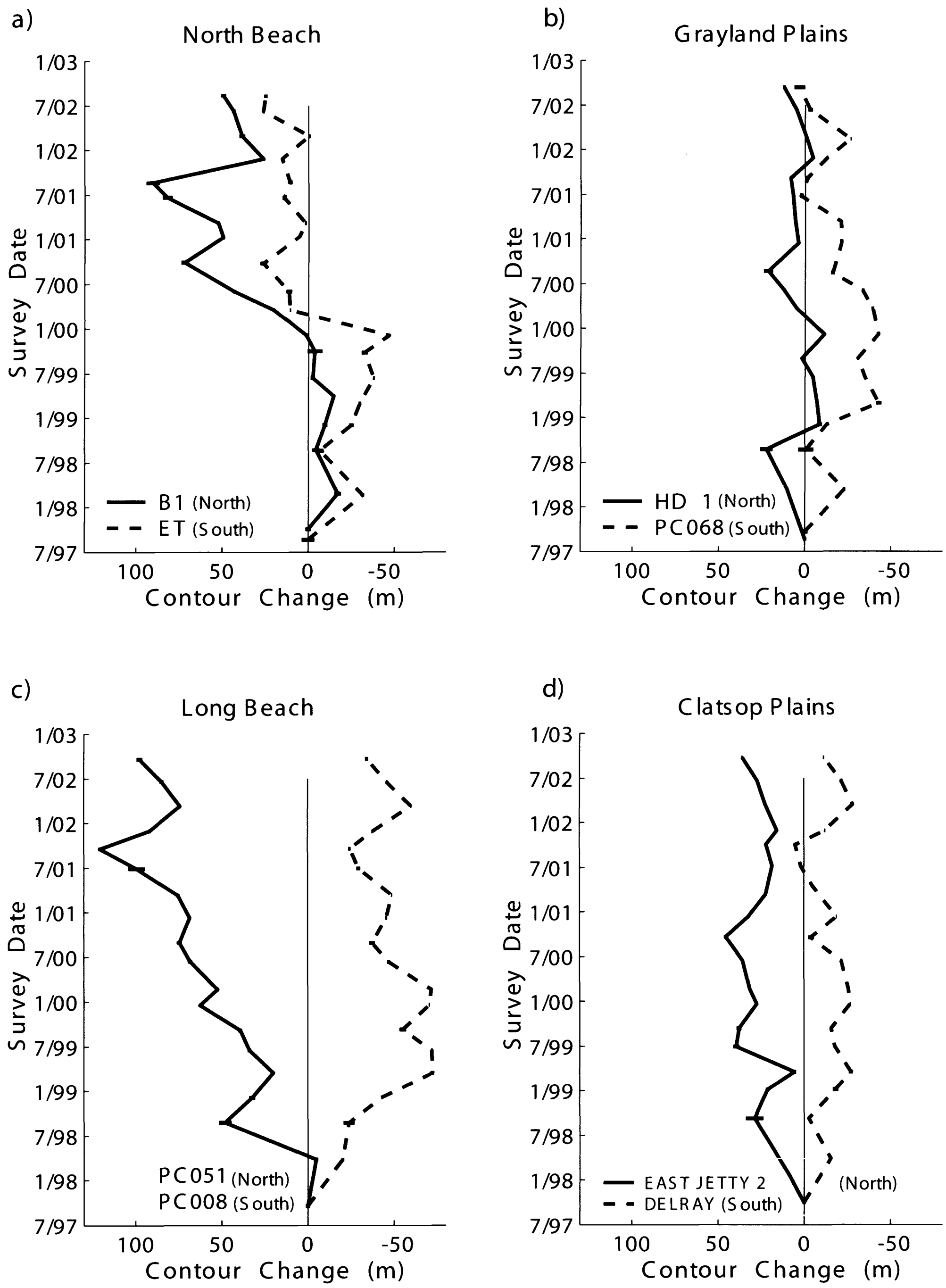

Figure 15. Time evolution of the 3.0-meter contour at beach profiles near the northern and southern limit of each subcell. Horizontal bars represent estimates of error bars on calculating the 3.0-meter contour.

where H_b is breaking wave height, ω is the incident band radian frequency ($2\pi/T$; T = the period), g is the acceleration of gravity, tan β is the beach/surf zone gradient, $\omega_{seconds}$ is the sediment fall velocity, and MSR is the mean spring tide range. Combining long-term records (~20 years) of monthly mean wave heights and periods (Table 1) with 5 years of beach morphology data reveals that CRLC beaches virtually never depart from a fully dissipative modal beach state. With the use of a spatial and temporal mean CRLC beach slope (0.02) and median grain size (0.18 mm), monthly mean values of ϵ and Ω average 132 (ranging from 116 to 155, SD = 10) and 11.1 (ranging from 8.4 to 14.4, SD = 2.1), respectively. The dissipative extreme according to WRIGHT and SHORT (1983, 1984) is characterized by an ϵ ranging from 30 to over

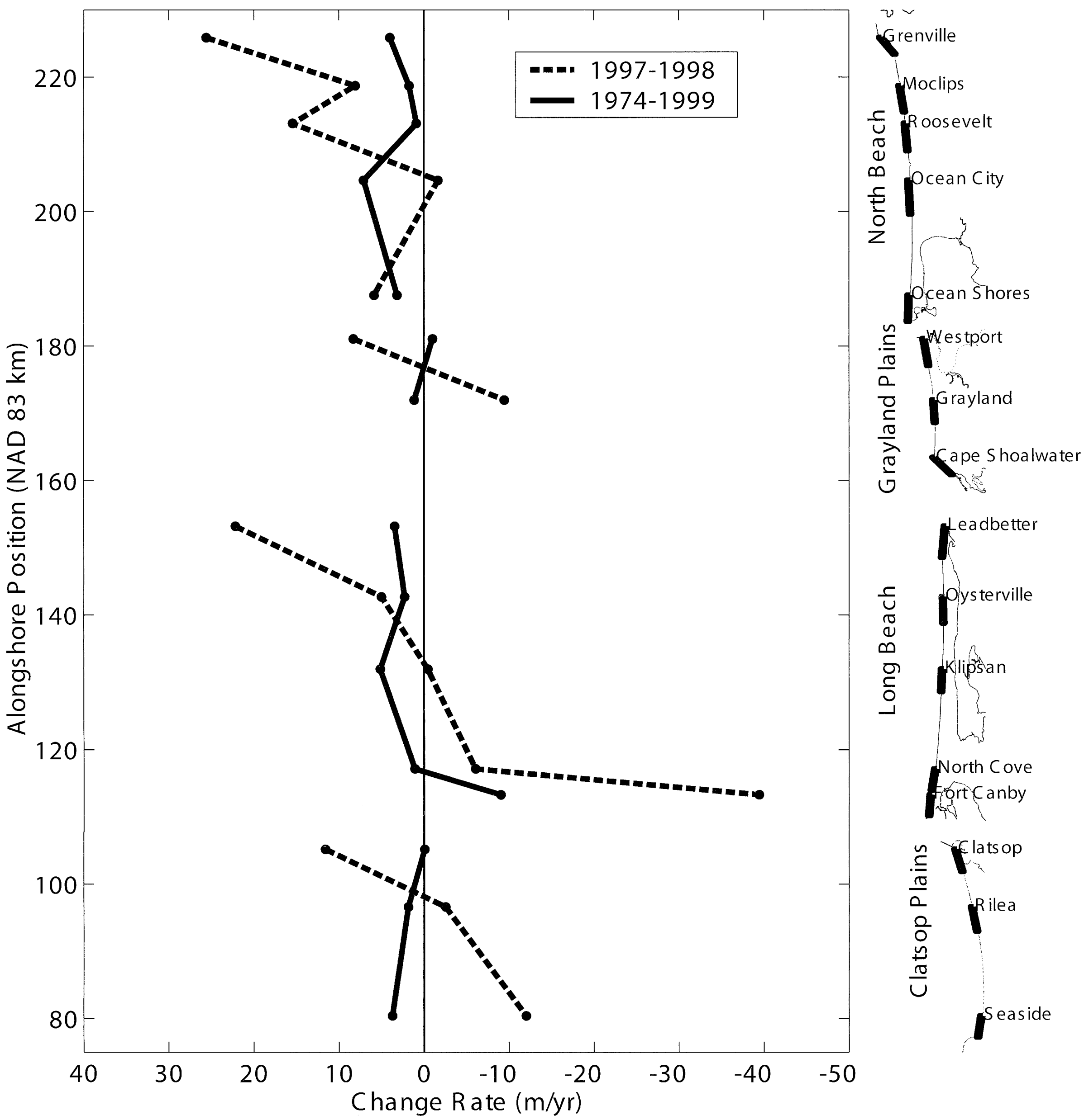

Figure 16. Alongshore-averaged change of the 3.0-meter contour at 15 of the 16 beach surface maps between summer 1997 and summer 1998 illustrating the regional beach response to the El Niño. Decadal-scale shoreline change rates (1974–1999), calculated over the same alongshore extents as the surface maps, are shown for comparison.

100 and an Ω ranging from 6 to 30. Monthly mean values of RTR average 1.3, ranging from 0.8 to 2.0 (SD = 0.4), placing CRLC beaches within the barred dissipative beach refined classification of MASSELINK and SHORT (1993).

According to the WRIGHT and SHORT (1983, 1984) classification, fully dissipative beaches in Australia exhibit very low gradients and have wide multibarred surf zones, with spilling breaking waves and infragravity energy dominating the surf zone. The beaches of the CRLC demonstrate similar characteristics with a few notable differences. First, the sandbars within the CRLC are often quite pronounced, particularly along the Long Beach subcell, where in 1999, the outer sandbar height averaged approximately 4.0 meters over 20 kilometers of measurements. These observations contrast with the assertion of MASSELINK and SHORT (1993) that dissipative beaches (at least in Australia) exhibit subdued sandbar morphologies. The large amplitude of offshore sandbars found in the CRLC also contrasts with the classification scheme that was based on observations at the FRF of LIPPMAN and HOLMAN (1990), who correlated the dissipative extreme of WRIGHT and SHORT (1984) with an unbarred surf zone. Second, longshore rhythmic morphology is often present

Table 4. *Alongshore-averaged change rates of the 3.0-m contour (NAVD 88) calculated from each of the 16 topographic beach surface maps.*

Surface Map No.	Surface Map Name	Winter Retreat (m)	Summer Recovery (m)	Net Change Rate 1997–2002 (m/y)	Shoreline Change 1974–1999 (m/y)
1	Grenville	−17.5	21.3	3.8	4.0
2	Moclips	−18.9	24.2	5.4	1.8
3	Roosevelt	−14.8	18.3	3.6	0.9
4	Ocean City	−22.5	22.1	−0.5	7.1
5	Ocean Shores	−24.2	28.6	4.4	3.1
6	Westport	−11.9	11.1	−0.8	−1.0
7	Grayland	−19.5	19.6	0.0	1.1
8	Cape Shoalwater*	−30.8	11.4	−19.3	—
9	Leadbetter	−5.8	28.4	22.6	3.5
10	Oysterville	−20.4	23.2	2.7	2.3
11	Klipsan	−15.0	19.1	4.2	5.2
12	North Head	−21.3	17.3	−4.0	1.1
13	Ft. Canby	−35.5	29.0	−6.5	−9.0
14	Clatsop	−14.5	16.6	2.1	−0.1
15	Rilea	−13.7	11.5	−2.2	1.9
16	Seaside	−19.8	15.7	−4.1	3.7
	Mean	−18.4	20.4	2.0	1.7
	SD	6.7	5.7	6.7	3.6
	Maximum	−5.8	29.0	22.6	7.1
	Minimum	−35.5	11.1	−6.5	−9.0

* Cape Shoalwater surface map data is not included in the calculations of regional statistics because of the influence of inlet processes at Willapa Bay.

along the CRLC, whereas longshore rhythms or significant irregularities are rarely present on dissipative Australian beaches (WRIGHT and SHORT, 1984). Rhythmicity within the CRLC occurs in both nearshore bathymetry, as illustrated by the crescentic middle sandbar located offshore from Oysterville in 1999 (Figure 7c), and in subaerial topography (Figure 6d), in which rhythmic, low-amplitude megacusps are ubiquitous within the CRLC during the spring and summer.

Another feature of the beaches within the CRLC that contrasts with previous classification schemes is the oblique onshore migrating intertidal slip-face ridges that dominate the beach face during the spring-summer recovery phase of the seasonal cycle, even though they are consistently dissipative over the full surf zone. In the classification of WRIGHT and SHORT (1984), ridge-runnel topography is an intermediate stage closer to the reflective than to the dissipative end member. In the CRLC, the development, onshore migration, and welding of intertidal bars to the upper beach face is believed to be the primary morphodynamic mechanism for subaerial beach growth and shoreline progradation on a seasonal scale. The majority of beaches along the CRLC exhibited net residual progradation of several meters per year over the 5-year duration of the monitoring program, as well as significant progradation rates over the historical (up to tens of meters per year; KAMINSKY *et al.,* 1999) and late geological periods (~0.5 m/y; WOXELL, 1998). Therefore, a detailed understanding of the accretionary phase of the morphodynamic cycle will be a focus of future investigations.

Morphodynamic Effects of El Niño and La Niña

During the 1997/1998 El Niño, US Pacific Northwest beaches experienced monthly mean water levels up to 0.4 meter higher than typical (Figure 3), monthly mean winter wave heights up to 1.0 meter higher than usual, and wave directions with a more southwest approach than typical (KAMINSKY, RUGGIERO, and GELFENBAUM, 1998; KOMAR *et al.,* 2000; REVELL, KOMAR, and SALLENGER, 2002). Although monthly mean water levels and wave directions were closer to normal during the 1998/1999 La Niña, this event brought an increased number of storms to the region, with higher wave conditions and more significant storm surges than previously experienced (ALLAN and KOMAR, 2002). These changes in environmental conditions because of interannual climatic variability had a distinct morphological effect on CRLC beaches (Figures 15 and 16). KOMAR *et al.* (2000) and ALLAN and KOMAR (2002) calculated the run-up of waves on beaches from the largest storms occurring during these two winters. The run-up estimates were added to the measured tides to yield total water elevations during the storms. These analyses confirm that the major storms during both the El Niño and the La Niña yielded total water levels that were sufficient to account, at least qualitatively, for the observed erosion.

The anomalous environmental conditions associated with the 1997/1998 El Niño, in particular waves approaching more from the southwest between June and October 1997 (Figure 3), resulted in a higher than typical annual net northward sediment transport. Although northward-directed sediment transport was higher than typical during winter 1997/1998 because of relatively large waves, CRLC beaches were preconditioned to erode in the southern end of subcells because of a reduction in southerly-directed sediment transport during the previous summer. Comparing the annual 1997 to 1998 shoreline change rates with the long-term shoreline change rates from 1974 to 1999 indicates significant sediment accumulation, beyond the long-term trends, at the northern boundaries of each subcell (Figure 16). The anomalous El Niño sediment transport patterns forced this subcell shoreline reorientation. However, the pattern of longshore transport necessary to cause these observed changes could

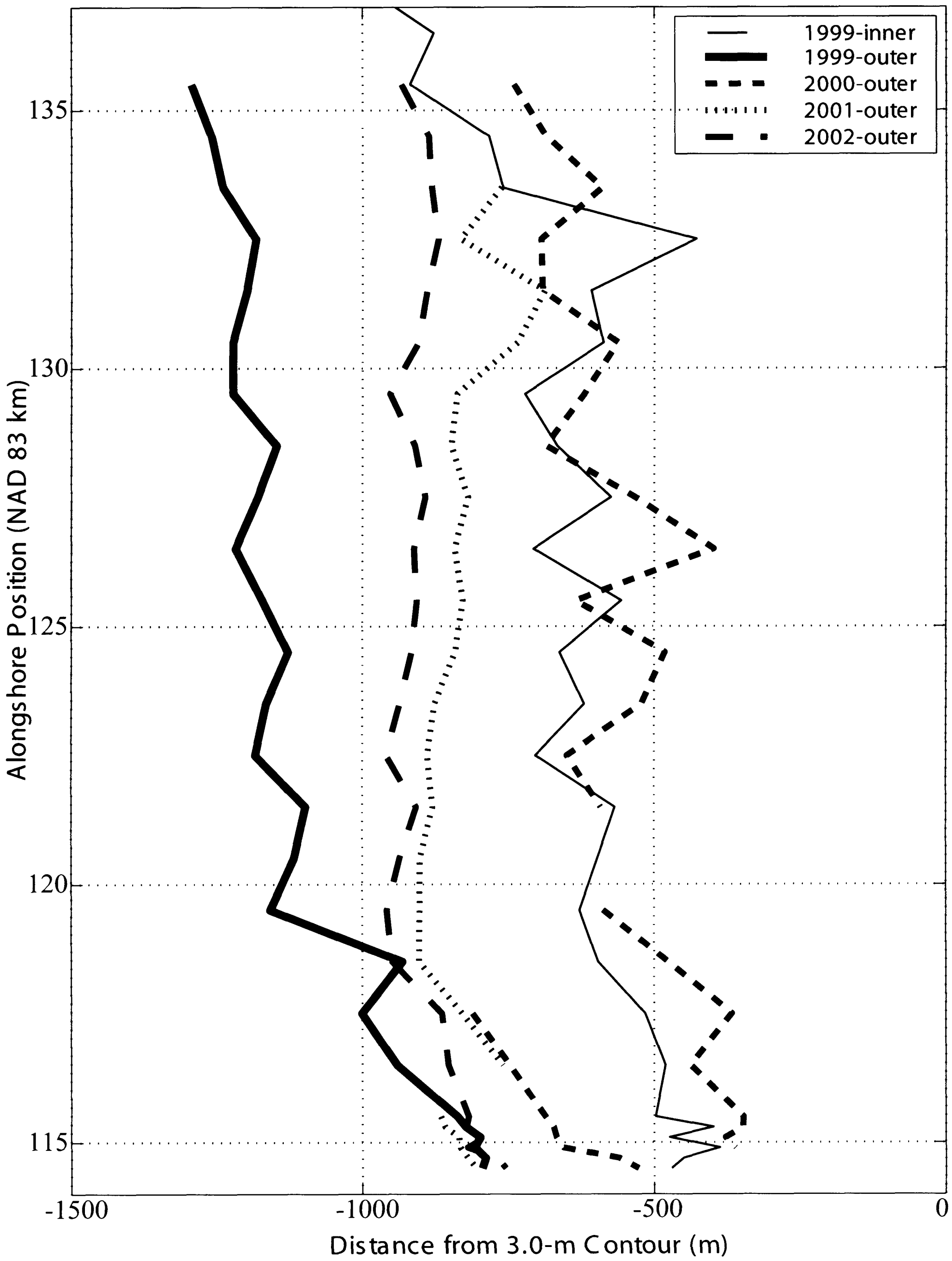

Figure 17. Evolution of the position of the outer sandbar, relative to the 3.0-meter contour position, along the Long Beach subcell from 1999 to 2002.

not be reproduced by a one-line shoreline change model without the inclusion of a sediment sink accounting for significant cross-shore losses (BUIJSMAN, RUGGIERO, and KAMINSKY, 2001). The increase in offshore-directed sediment transport relative to normal conditions was probably the result of both increased wave heights and higher than normal water levels. Therefore, both model results and morphology change measurements suggest that although strong gradients in longshore transport are necessary to force the observed subcell shoreline reorientation, the overall morphological change associated with the 1997/1998 El Niño was the result of a combination of both cross-shore and longshore processes.

During the moderate La Niña of 1998/1999, four storms produced deep-water significant wave heights greater than 10 meters (ALLAN and KOMAR, 2002), with the largest event on record occurring on 2–3 March 1999, producing 14.1-meter significant wave heights. Between summer 1998 and summer 1999, CRLC shorelines retreated 9 meters on average (ranging from 6 meters of progradation to 26 meters of retreat, SD = 9 meters). Unlike during the 1997/1998 El Niño, no strong alongshore gradient in subaerial beach response is evident in the La Niña contour change signal (not shown). The strength of La Niña–induced gradients in cross-shore sediment transport is evidenced by changes in nearshore bathymetry between 1998 and 1999. The alongshore-averaged outer sandbar height, along a 3-kilometer stretch of Long Beach Peninsula, increased from 0.6 meter (from crest to trough) in summer 1998 to approximately 3.5 meters in summer 1999 (Figure 7d). In contrast to strong El Niños, it appears that cross-shore processes dominate the morphological response of the CRLC during La Niña events.

CONCLUSIONS

The beach morphology monitoring program of the SWCES has for the first time comprehensively and systematically quantified the short- to medium-term morphodynamic variability of the 165-kilometer-long Columbia River littoral cell. The sampling scheme, nested both in time and space, successfully resolved the seasonal cycle of beach loss and recovery. Variations in upper shoreface slopes, foredune ridge morphologies, and sandbar dimensions document the extent of alongshore variability in large-scale coastal behavior not previously known to exist in US Pacific Northwest littoral cells or on high-energy dissipative beaches in general.

The seasonal exchange of sand between the onshore and offshore is considerable. Relatively high winter waves and water levels force offshore and northerly sediment transport, resulting in subaerial beach lowering on the order of 0.5 meter while the shoreline retreats horizontally between 10 and 40 meters. Onshore and weak southerly sediment transport dominates beach recovery in the summer months. The alongshore spacing of topographic beach profiles and surface maps quantified the large-scale shoreline reorientation because of an interannual climatic fluctuation, the El Niño event of 1997/1998. The observed morphological response to the 1997/1998 El Niño event was a result of both anomalous alongshore and cross-shore gradients in sediment transport. In contrast, cross-shore processes dominated the morphological response ($\sim$10 meters of net erosion throughout the littoral cell) to the 1998/1999 La Niña. The interannual variability within the CRLC for 1997 to 2002 is large, with shoreline change rates of up to approximately 10 m/y, a variability that can mask longer term shoreline change trends.

Continued research on the variability in beach behavior across multiple scales is important for both an improved understanding of large-scale coastal behavior and coastal management decision making. For example, in several locations, recent trends in shoreline change are in the opposite direction to longer term historical trends, a result that has serious implications for developing a predictive capability at decadal scales. Furthermore, the monitoring program alone cannot resolve the regional morphological response to long-term climate change signals evident in either increasing wave heights (ALLAN and KOMAR, 2000), relative sea level rise, or Pacific decadal oscillation cycles. The integration of data from the beach monitoring program with geological and oceanographic data sets allows researchers to develop conceptual and numerical models of regional coastal behavior. Although important alongshore differences in subregional coastal behavior have been found, future work aims to examine the primary causative processes (*e.g.,* sediment supply, shoreface morphology, and wave climate) responsible for these differences.

ACKNOWLEDGMENTS

This work was funded by the US Geological Survey (USGS), the Washington Department of Ecology, and the USGS Mendenhall Postdoctoral Fellowship Program. We thank Laura Bauleke, Jessica Côté, Dawn Harpel, Laura Kerr, Etienne Kingsley, Emily Lindstrum, Diana McCandless, Josh McInnes, Jamie MacMahan, David Thompson, and Troy Warnick, who collected the bulk of the data. Maarten Buijsman, Rich Daniels, Steve Eykelhoff, Bob Huxford, Sarah Haque, Dylan Monahan, and Peter Wald were always available when necessary to make sure that we "got the data." This manuscript benefited significantly from the comments of Paul Komar, Abby Sallenger, and two anonymous reviewers.

LITERATURE CITED

ALLAN, J.C. and KOMAR, P.D., 2000. Are ocean wave heights increasing in the eastern North Pacific? *EOS, Transactions of the American Geophysical Union,* 47, 561–567.

ALLAN, J.C. and KOMAR, P.D., 2002. Extreme storms in the Pacific Northwest coast during the 1997–98 El Niño and 1998–99 La Niña. *Journal of Coastal Research,* 18(1), 175–193.

ATWATER, B.F.; NELSON, A.R.; CLAQUE, J.J.; YAMAGUCHI, D.K.; DOBROWSKY, P.T.; BOURGEOIS, J.; DARIENZO, M.E.; GRANT, W.C.; HEMPHILL-HALEY, E.; KELSEY, H.M.; JACOBY, G.C; NICHENKO, S.P.; PALMER, S.P.; PETERSON, C.D., and REINHART, M.A., 1995. Summary of coastal geological evidence for past great earthquakes at the Cascadia subduction zone. *Earthquake Spectra,* 11, 1–18.

BEACH, R.A.; HOLMAN, R.A., and STANLEY, J., 1996. Measuring nearshore bathymetry on high energy beaches. Presented at the American Geophysical Union Fall Meeting. *EOS Transactions of the American Geophysical Union,* F286.

BIRKEMEIR, W.A., 1985. Time scales of nearshore profile change. *In*: Proceedings of the 19th International Conference on Coastal Engineering, ASCE, pp. 1507–1521.

BUIJSMAN, M.C.; KAMINSKY, G.M., and GELFENBAUM, G., 2003. Shoreline change associated with jetty construction, deterioration, and rehabilitation at Grays Harbor, Washington. *Shore and Beach,* 71, 15–22.

BUIJSMAN, M.C.; RUGGIERO, P., and KAMINSKY, G.M., 2001. Sensitivity of shoreline change predictions to wave climate variability along the southwest Washington coast, USA. *In*: Proceedings of Coastal Dynamics '01, ASCE, pp. 617–626.

COTE, J.M., 1999. The measurement of nearshore bathymetry on intermediate and dissipative beaches. Corvallis, Oregon: Oregon State University, Master's thesis, 102p.

CROWELL, M.; LEATHERMAN, S.P., and BUCKLEY, M.K., 1991. Historical shoreline change: error analysis and mapping accuracy. *Journal of Coastal Research,* 7(3), 839–852.

DANIELS, R.C.; RUGGIERO, P., and WEBER, L.E., 1999. Washington Coastal Geodetic Control Network: Report and Station Index. Olympia, Washington: Washington Department of Ecology Publication #99-103, 268p.

DEAN, R.G., 1973. Heuristic models of sand transport in the surf zone. *In*: Proceedings of Conference on Engineering Dynamics in the Surf Zone, Sydney, N.S.W., pp. 208–214.

DOLAN, R.; HAYDEN, B.P., and HEYWOOD, J., 1978. A new photogrammetric method for determining shoreline erosion. *Coastal Engineering,* 2, 21–39.

DOUGLAS, B.C. and CROWELL, M., 2000. Long-term shoreline position prediction and error propagation. *Journal of Coastal Research,* 16(1), 145–152.

GAYES, P.T.; BALWIN, W.; VAN DOLAH, R.F.; JUTTE, P.; EISER, W.C., and HANSEN, N., 2001. Systematic coastal monitoring: the S. Carolina coast (USA). *In*: Proceedings of Coastal Dynamics '01, ASCE, pp. 868–877.

GELFENBAUM, G.; SHERWOOD, C.R.; PETERSON, C.; KAMINSKY, G.M.; BUIJSMAN, M.C.; TWICHELL, D.C.; RUGGIERO, P.; GIBBS, A.E., and REED, C., 1999. The Columbia River littoral cell: a sediment budget overview. *In*: Proceedings of Coastal Sediments '99, ASCE, pp. 1660–1675.

GELFENBAUM, G.; BUIJSMAN, M.C.; SHERWOOD, C.R.; MORITZ, H.R., and GIBBS, A.E., 2001. Coastal evolution and sediment budget at the mouth of the Columbia River, USA. *In*: Proceedings of Coastal Dynamics '01, ASCE, pp. 818–827.

GORMAN, L.; MORANG, A., and LARSON, R., 1998. Monitoring the coastal environment; part IV: mapping, shoreline changes, and bathymetric analysis. *Journal of Coastal Research,* 14(1), 61–92.

GUZA, R.T. and INMAN, D.L., 1975. Edge waves and beach cusps. *Journal of Geophysical Research,* 80(21), 2997–3002.

HESP, P., 2002. Foredunes and blowouts: initiation, geomorphology and dynamics. *Geomorphology,* 48, 245–268.

KAMINSKY, G.M. and GELFENBAUM, G., 1999. The southwest Washington coastal erosion study: research in support of coastal management. *Coastal Zone '99,* 737–739.

KAMINSKY, G.M.; RUGGIERO, P., and GELFENBAUM, G., 1998. Monitoring coastal change in southwest Washington and northwest Oregon during the 1997/98 El Niño. *Shore & Beach,* 66(3), 42–51.

KAMINSKY, G.M.; RUGGIERO, P.; GELFENBAUM, G., and PETERSON, C., 1997. Long-term coastal evolution and regional dynamics of a US Pacific Northwest littoral cell. *In*: Proceedings of Coastal Dynamics '97, ASCE, pp. 614–623.

KAMINSKY, G.M.; DANIELS, R.; HUXFORD, B.; MCANDLESS, D., and RUGGIERO, P., 1999a. Mapping erosion hazard areas in Pacific County, Washington. *Journal of Coastal Research, Special Issue* 28, 158–170.

KAMINSKY, G.M.; BUIJSMAN, M.C.; GELFENBAUM, G.; RUGGIERO, P.; JOL, H.M.; GIBBS, A.M., and PETERSON, C., 1999b. Synthesizing geological observations and processes—response data for modeling coastal change at management scale. *In*: Proceedings of Coastal Sediments '99, ASCE, pp. 1708–1723.

KOMAR, P.D., 1986. The 1982–83 El Niño and erosion on the Oregon coast. *Shore and Beach,* 54, 3–12.

KOMAR, P.D., 1998. *Beach Processes and Sedimentation,* 2nd edition. Englewood Cliffs, New Jersey: Prentice Hall, 544p.

KOMAR, P.D.; ALLAN, J.C.; DIAS-MENDEZ, G.; MARRA, J.J., and RUGGIERO, P., 2000. El Niño and La Niña—erosion processes and impacts. *In*: Proceedings of the 27th International Conference on Coastal Engineering, ASCE, pp. 2414–2427.

LARSON, R.; MORANG, A., and GORMAN, L., 1997. Monitoring the coastal environment; part II: sediment sampling and geotechnical methods. *Journal of Coastal Research,* 12(2), 308–330.

LI, M.Z. and KOMAR, P.D., 1991. Longshore grain sorting and beach placer formation adjacent to the Columbia River. *Journal of Sedimentary Petrology,* 62(3), 429–441.

LIPPMAN, T.C. and HOLMAN, R.A., 1990. The spatial and temporal variability of sand bar morphology. *Journal of Geophysical Research,* 95(C7), 11575–11590.

LIPPMAN, T.C.; HOLMAN, R.A., and HATHAWAY, K.K., 1993. Episodic, non-stationary behavior of a double bar system at Duck, NC, USA, 1986–1991. *Journal of Coastal Research,* SI 15, 49–75.

LIST, J.H. and FERRIS, A.S., 1998. Regional-scale shoreline response to storms. Presented at the American Geophysical Union Fall Meeting. *EOS Transactions of the American Geophysical Union,* F445.

MACMAHAN, J., 2001. Hydrographic surveying from a personal watercraft. *Journal of Surveying Engineering,* 127(1), 12–24.

MASSELINK, G. and SHORT, A.D., 1993. The effect of tide range on beach morphodynamics and morphology: a conceptual model. *Journal of Coastal Research,* 9(3), 785–800.

MEYERS, R.A.; SMITH, D.G.; JOL, H.M., and PETERSON, C.D., 1996. Evidence for eight great earthquake-subsidence events detected with ground penetrating radar, Willapa Barrier, Washington, *Geology,* 24(2), 99–102.

MORANG, A.; LARSON, R., and GORMAN, L., 1997. Monitoring the coastal environment; part I: waves and currents. *Journal of Coastal Research,* 13(1), 111–133.

MORTON, R.A., 1997. *Gulf Shoreline Movement between Sabine Pass and the Brazos River, Texas: 1974 to 1996.* Austin, Texas: Texas Bureau of Economic Geology Geological Circular 97-3, 46p.

MORTON, R.A. and SPEED, F.M., 1998. Evaluation of shorelines and legal boundaries controlled by water levels on sandy beaches. *Journal of Coastal Research,* 14(4), 1373–1384.

MORTON, R.A.; LEACH, M.P.; PAINE, J.G., and CARDOZA, M.A., 1993. Monitoring beach changes using GPS surveying techniques. *Journal of Coastal Research,* 9(3), 702–720.

OFFICE OF BEACHES AND COASTAL SYSTEMS, 2001. *Statewide Coastal Monitoring Program.* Tallahassee, Florida: (Florida) Department of Environmental Protection Report, 7p.

PETERSON, C.D.; JACKSON, P.L.; ONEILL, D.J.; ROSENFELD, C.L., and KIMERLING, A.J., 1990. Littoral cell response to interannual climatic forcing 1983–1987 on the central Oregon coast, USA. *Journal of Coastal Research,* 6(1), 87–110.

PETERSON, C.D.; DARIENZO, M.E.; HAMILTON, D.H.; PETTIT, D.H., and YEAGER, R.K., 1994. *Cascadia Beach-Shoreline Database, Pacific Northwest Region, USA.* State of Oregon Department of Geology and Mineral Resources Open File Report 0-94-2.

PETERSON, C.D.; GELFENBAUM, G.; JOL, H.M.; PHIPPS, J.B.; RECKENDORF, F.; TWICHEL, D.C.; VANDERBURG, S., and WOXELL, L.K., 1999. Great earthquakes, abundant sand, and high wave energy in the Columbia Cell, USA. *In*: Proceedings of Coastal Sediments '99, ASCE, pp. 1676–1691.

PLANT, N.G. and HOLMAN, R.A., 1997. Intertidal beach profile estimation using video images. *Marine Geology,* 140, 1–24.

PLANT, N.G.; HOLMAN, R.A., and FREILICH, M.H., 1999. A simple model for interannual sandbar behavior. *Journal of Geophysical Research,* 104(C7), 15755–15776.

REVELL, D.L.; KOMAR, P.D., and SALLENGER, A.H., 2002. An application of LIDAR to analyses of El Niño erosion in the Netarts littoral cell, Oregon. *Journal of Coastal Research,* 18(4), 792–801.

RUESSINK, B.G. and KROON, A., 1994. The behaviour of a multiple bar system in the nearshore zone of Terschelling, The Netherlands: 1965:1993. *Marine Geology,* 121, 187–197.

RUGGIERO, P.; KAMINSKY, G.M., and GELFENBAUM, G., 2003. Linking proxy-based and datum-based shorelines on high-energy coasts: implications for shoreline change analyses. *Journal of Coastal Research,* SI 38, 57–82.

RUGGIERO, P. and VOIGT, B., 2000. *Beach Monitoring in the Columbia River Littoral Cell, 1997–2000.* Olympia, Washington: Washington Department of Ecology Publication 00-06-26, 112p.

RUGGIERO, P.; KAMINSKY, G.M.; KOMAR, P.D., and MCDOUGAL, W.G., 1997. Extreme waves and coastal erosion in the Pacific Northwest. *In*: Proceedings of Waves '97, ASCE, pp. 947–961.

RUGGIERO, P.; COTE, J.; KAMINSKY, G.M., and GELFENBAUM, G., 1999. Scales of variability along the Columbia River littoral cell. *In*: Proceedings of Coastal Sediments '99, ASCE, pp. 1692–1707.

RUGGIERO, P.; GELFENBAUM, G.; THOMPSON, D., and KAMINSKY, G.M., 2001. Exploring the relationship between nearshore morphology and shoreline change. *In*: Proceedings of Coastal Dynamics '01, ASCE, pp. 627–636.

RUGGIERO, P.; GELFENBAUM, G.; SHERWOOD, C.R.; LACY, J., and BUIJSMAN, M.C., 2003. Linking nearshore processes and morphology measurements to understand large scale coastal change. *In*: Proceedings of Coastal Sediments '03, ASCE.

SALLENGER, A.H., JR.; KRABILL, W.B.; SWIFT, R.N.; BROCK, J.; LIST, J.; HANSEN, M.; HOLMAN, R.A.; MANIZADE, S.; SONTAG, J.; MEREDITH, A.; MORGAN, K.; YUNKEL, J.K.; FREDERICK, E.B., and STOCKDON, H., 2003. Evaluation of airborne topographic lidar for quantifying beach changes. *Journal of Coastal Research,* 19(1), 125–133.

SHAND; R.D.; BAILEY, D.G., and SHEPARD, M.J., 1999. An inter-site comparison of net offshore bar migration characteristics and environmental conditions. *Journal of Coastal Research,* 15(3), 750–765.

SHERWOOD, C.R.; GELFENBAUM, G.; HOWD, P.A., and PALMSTEN, M.L., 2001. Sediment transport on a high-energy ebb-tidal delta. *In*: Proceedings of Coastal Dynamics '01, ASCE, pp. 473–482.

SMITH, G.L. and ZARILLO, G.A., 1990. Calculating long-term shoreline recession rates using aerial photographic and beach profiling techniques. *Journal of Coastal Research,* 1, 111–120.

STOCKDON, H.F.; SALLENGER, A.H.; LIST, J.H., JR., and HOLMAN, R.A., 2002. Estimation of shoreline position and change using airborne topographic lidar data. *Journal of Coastal Research,* 18(3), 502–513.

TETRA TECH INC., 1986. *Recommended Protocols for Measuring Conventional Sediment Variables in Puget Sound.* Report prepared for the US Environmental Protection Agency, 46p.

TILLOTSEN, K.J. and KOMAR, P.D., 1997. The wave climate of the Pacific Northwest (Oregon and Washington): a comparison of data sources. *Journal of Coastal Research,* 13, 440–452.

TRIMBLE NAVIGATION LIMITED, 1998. *4700 Receiver Operation Manual,* version 1.0, part number 36238-00, revision B.

VAN RIGN, L.C.; WALSTRA, D.J.R.; GRASMEIJER, B.; SUTHERLAND, J.; PAN, S., and SIERRA, J.P., 2003. The predictability of cross-shore bed evolution of sandy beaches at the time scale of storms and seasons using process-based Profile models. *Coastal Engineering,* 47, 295–327.

WIJNBERG, K.M., 2002. Environmental controls on decadal morphologic behaviour of the Holland coast. *Marine Geology,* 189, 227–247.

WIJNBERG, K.M. and KROON, A., 2002. Barred beaches. *Geomorphology,* 48, 103–120.

WOXELL, L.K., 1998. Prehistoric beach accretion rates and long-term response to sediment depletion in the Columbia River littoral system, USA. Portland, Oregon: Portland State University, Master's thesis, 206p.

WRIGHT, L.D. and SHORT, A.D., 1983. Morphodynamics of beaches and surf zones in Australia. *In*: KOMAR, P.D. (ed.), *Handbook of Coastal Processes and Erosion.* Boca Raton, Florida: CRC Press, pp. 35–64.

WRIGHT, L.D. and SHORT, A.D., 1984. Morphodynamic variability of surf zones and beaches: a synthesis. *Marine Geology,* 56, 93–118.

ZILKOSKI, D.B.; D'ONOFRIO, J.D., and FRAKES, S.J., 1997. *Guidelines for Establishing GPS-Derived Ellipsoid Heights (Standards: 2 centimeters and 5 centimeters),* version 4.3. Silver Springs, Maryland: NOAA Technical Memorandum, NOS NGS-58.